Phenological assessment of transpiration: The stem-temp approach for determining start and end of season

Magali F. Nehemy [a,b,c,*], Zoe Pierrat [d], Jason Maillet [b,e], Andrew D. Richardson [f,g], Jochen Stutz [d,h], Bruce Johnson [a,h], Warren Helgason [a,f,h], Alan G. Barr [a,h], Colin P. Laroque [a,b,h], Jeffrey J. McDonnell [a,i,h]

[a] Trent School of the Environment, Trent University, Peterborough, Canada
[b] Mistik Askiwin Dendrochronology Laboratory (MAD Lab), University of Saskatchewan, Saskatoon, Canada
[c] Global Institute for Water Security, University of Saskatchewan, Saskatoon, Canada
[d] Department of Atmospheric and Oceanic Sciences, University of California Los Angeles, Los Angeles, United States
[e] Department of Geography, The University of Winnipeg, Winnipeg, Canada
[f] Center for Ecosystem Science and Society, Northern Arizona University, Flagstaff, United States
[g] School of Informatics, Computing, and Cyber Systems, Northern Arizona University, Flagstaff, United States
[h] Department of Civil, Geological, and Environmental Engineering, University of Saskatchewan, Saskatoon, Canada
[i] School of Geography, Earth and Environmental Sciences, University of Birmingham, Birmingham, United Kingdom

ARTICLE INFO

ABSTRACT

Field-based assessment of transpiration phenology in boreal tree species is a significant challenge. Here we develop an objective approach that uses stem radius change and its correlation with sapwood temperature to determine the timing of phenological changes in transpiration in mixed evergreen species. We test the *stem-temp* approach using a five year stem-radius dataset from black spruce (*Picea mariana*) and jack pine (*Pinus banksiana*) trees in Saskatchewan (2016–2020). We further compare transpiration phenological transition dates from this approach with tower-based phenological assessment from green chromatic coordinate derived from phenocam images, eddy-covariance-derived evapotranspiration and carbon uptake, tower-based measurements of solar-induced chlorophyll fluorescence and snowmelt timing. The stem-temp approach identified the start and end of four key transpiration phenological phases: (i) the end of temperature-driven cycles indicating the start of biological activity, (ii) the onset of stem rehydration, (iii) the onset of transpiration, and (iv) the end of transpiration-driven cycles. The proposed method is thus useful for characterizing the timing of changes in transpiration phenology and provides information about distinct processes that cannot be assessed with canopy-level phenological measurements alone.

1. Introduction

The timing of vegetation phenological transition dates (e.g., leaf-out, dormancy) drives functional changes in forest carbon and water cycles (Fitzjarrald et al., 2001; Keenan et al., 2014; Richardson et al., 2013, Richardson et al., 2010; Schwartz and Crawford, 2001; Wolf et al., 2016). For example, springtime vegetation phenology is recognized as one of the key determinants of the annual carbon (C) balance of temperate and boreal forest stands (Barr et al., 2007; Berninger, 1997; Black et al., 2000; Goulden et al., 1996). Therefore, quantifying the timing of vegetation phenological events is fundamental for understanding how climate change will influence shifts in the timing of water availability through earlier spring snowmelt (i.e., snow phenology) (Chen et al., 2015), increased length of the growing season—the length of period of the year when vegetation is active, transpiring and photosynthesizing—and later fall senescence (Barichivich et al., 2013; Linderholm, 2006; Menzel and Fabian, 1999).

In the boreal forest, biological activity is marked by climate seasonally. The biological awakening from dormancy in the spring corresponds closely to changes in environmental conditions, such as increase in air temperature, soil warming and thawing (Ahmed et al., 2021; Black et al., 2000; Goulden et al., 1996; Jarvis and Linder, 2000).

With the increase in soil temperatures and thawing in the spring, liquid water becomes available, and trees start to rehydrate their stems, transpire, and uptake carbon (Bowling et al., 2018; Nehemy et al., 2022; Pierrat et al., 2021). Transpiration and carbon uptake continues throughout the growing season until the fall when environmental conditions change. The decrease in air temperature and photoperiod in the fall induce physiological cold acclimation and leads to cessation of transpiration and carbon uptake (Chang et al., 2021). Despite the importance of accurately determining the timing of vegetation phenology phases, doing so quantitatively has remained a significant challenge for both models and measurements (Commane et al., 2017; Parazoo et al., 2018; Peng et al., 2015; Pierrat et al., 2021; Richardson et al., 2012). Multiple approaches can provide phenological information needed for understanding the multi-day transition associated with changes in photosynthetic activity and the transpiration process. For instance, eddy-covariance derived evapotranspiration (ET) provides information on water fluxes, but ET is subject to significant uncertainties and data gaps associated with measurement and calculation techniques (Baldocchi, 2003; Wutzler et al., 2018). These issues are especially problematic during shoulder seasons (e.g., transition from winter to spring and fall to winter). Additionally, ET is spatially averaged and includes understory, and thus unable to capture species-specific phenological change. Remotely sensed products such as solar-induced chlorophyll fluorescence (SIF), the chlorophyll-carotenoid index (CCI), and the green-chromatic coordinate (G_{CC}), among others, have all been valuable approaches to indicate the onset of biological activity in the spring (e.g., Gamon et al., 2016; Magney et al., 2019; Parazoo et al., 2018; Pierrat et al., 2021; Richardson et al., 2018). However, these measurements often provide start-of-season and end-of-season dates with uncertainties on the order of weeks (Parazoo et al., 2018; Walther et al., 2018) and do not necessarily provide information about the same physiological processes occurring within the plants (e.g., respiratory recycling of CO_2, transpiration, and photosynthesis) (Pierrat et al., 2021). This uncertainty (i.e., partitioning method of eddy covariance flux and the presence of snow cover in the canopy for remotely sensed products) limits our ability to mechanistically assess the observed changes and phenological responses of specific processes (e.g., transpiration, photosynthesis, carbon uptake) to environmental drivers.

We need a more accurate assessment of the onset of transpiration in the spring and when trees cease transpiration in the fall to improve our understanding of shifts in timing of transpiration phenological transition dates and potential interactions among environmental drivers (Fitzjarrald et al., 2001; Schwartz and Crawford, 2001); ideally, something simple that provides daily field-based measurements at the individual tree level so that the timing of the transition dates can be quantified within and between species. While continuous measurements of stem radius changes using automated dendrometers have been used to provide proxy data for tree water relations at high-temporal resolution (De Swaef et al., 2015; Drew and Downes, 2009; Zweifel et al., 2016), the potential of these data has not been fully explored yet to assess phenological changes in transpiration (e.g., the onset of stem rehydration and transpiration in the spring).

Seasonal changes in stem diurnal cycles throughout the year recorded using dendrometers have been previously observed (King et al., 2013). Sevanto et al. (2006) used transpiration-driven cycle patterns to detect transpiration and photosynthetic activity during specific warm winter days. Turcote et al. (2009) defined the seasonal occurrence of freeze-thaw cycles based on specific air temperature thresholds. However, determining when exactly the freeze-thaw cycle ceases and the transpiration-driven cycle begins is difficult (Sevanto et al., 2006). Additionally, air temperature and tissue temperature can differ due to the thermal inertia of wood. Specific sap freezing points can be variable given changes in tissue osmotic potential (Charrier et al., 2017).

What is critically needed to advance observation in transpiration phenology is an objective, dynamic metric that considers daily changes in sapwood temperature and diurnal radial change to evaluate shifts from freeze-thaw cycles to transpiration-driven cycles. Such an approach could provide a more exact assessment of the timing of transpiration phenological events (Commane et al., 2017; Parazoo et al., 2018; Peng et al., 2015; Pierrat et al., 2021; Richardson et al., 2012). Here we explore stem diurnal cycle observations as a means to provide direct evidence of transpiration phenology. This tree phenological monitoring can complement other canopy-level phenological assessment of photosynthetic activity (e.g., CCI, SIF, 'greenness' index, GPP). Stem cycles occur daily and provide assessment of the water related signal of the stems (King et al., 2013). This information can indicate when and whether trees are transpiring. The daily assessment of stem cycle is critical because within the broad seasonal definition of stem cycles (e.g., Turcotte et al., 2009), there are days within each season (e. g., spring, winter) where trees may not be following the general pattern (i.e., trees might transpire during winter (Sevanto et al., 2006)). During the onset of stem rehydration and transpiration in the spring, there is greater variability in air temperature, which may result in alternation between days where trees are transpiring and days where frost can induce freeze stems and inhibit transpiration (Pierrat et al., 2021).

To overcome some challenges associated with phenological assessment of vegetation, specifically the timing of spring onset and fall senescence we develop a new approach to identify the timing of transpiration changes in the boreal forest using high frequency stem diurnal cycles. We test this new approach using high-resolution stem radius measurements and sapwood temperature, and air temperature, collected over five years (2016–2020) in two boreal forest sites in Saskatchewan, Canada, with distinct species composition. We combine this with canopy greenness assessment using green-chromatic coordinate (G_{CC}), tower measurements of solar-induced chlorophyll fluorescence (SIF), and eddy-covariance derived evapotranspiration (ET). Our objectives are to (1) define the timing of transpiration phenological changes in the boreal forest using a new stem cycle-sapwood temperature correlation approach (2) evaluate the new approach for black spruce (*Picea mariana*) and jack pine (*Pinus bankisiana*) trees growing in different sites, and (3) compare the timing of phenological events obtained from this newly proposed transpiration phenology assessment with a well-established assessment of canopy-level phenological changes (G_{CC}).

2. Theory and approach

The theory behind our stem diurnal cycle approach is based on many years of research from the scientific community. The water-related shrinkage and refilling signal of the stem reflects daily changes in the water balance of elastic tissues (Irvine and Grace, 1997; Kozlowski and Winget, 1964) and can be isolated from the growth signal (Zweifel et al., 2016). During summer, tree stems shrink during the day because of the negative water potential gradients generated by transpiration which results in the radial water transfer from elastic inner bark tissues (phloem and cambium) to the xylem conduits (Perämäki et al., 2001; Steppe et al., 2006; Zweifel and Hasler, 2001). Conversely, stems expand at night and on rainy days because the water potential gradient reverses and water flows from the xylem back into the inner bark tissues, refilling internal storages. These responses result in stem shrinkage and expansion and characterize the transpiration-driven cycles driven by water potential gradients (Zweifel and Häsler, 2000). When trees are transpiring, the maximum radius is observed in the morning and minimum in the afternoon (Fig. 1b).

The stem diurnal cycle shows a reversed pattern during winter (Fig. 1a) compared to the transpiration-driven cycles (Fig. 1b) (Améglio et al., 2001; Charra-Vaskou et al., 2016; Maruta et al., 2020; Sevanto et al., 2006; Zweifel and Häsler, 2000). When air temperature drops to near freezing values , stem radius change is no longer controlled by transpiration. Instead, the radial changes start to synchronize with changes in air temperature. When the air temperature drops below freezing, ice starts to form in the xylem while the sap in the inner bark remains liquid (Améglio et al., 2001; Charrier et al., 2017) and stem
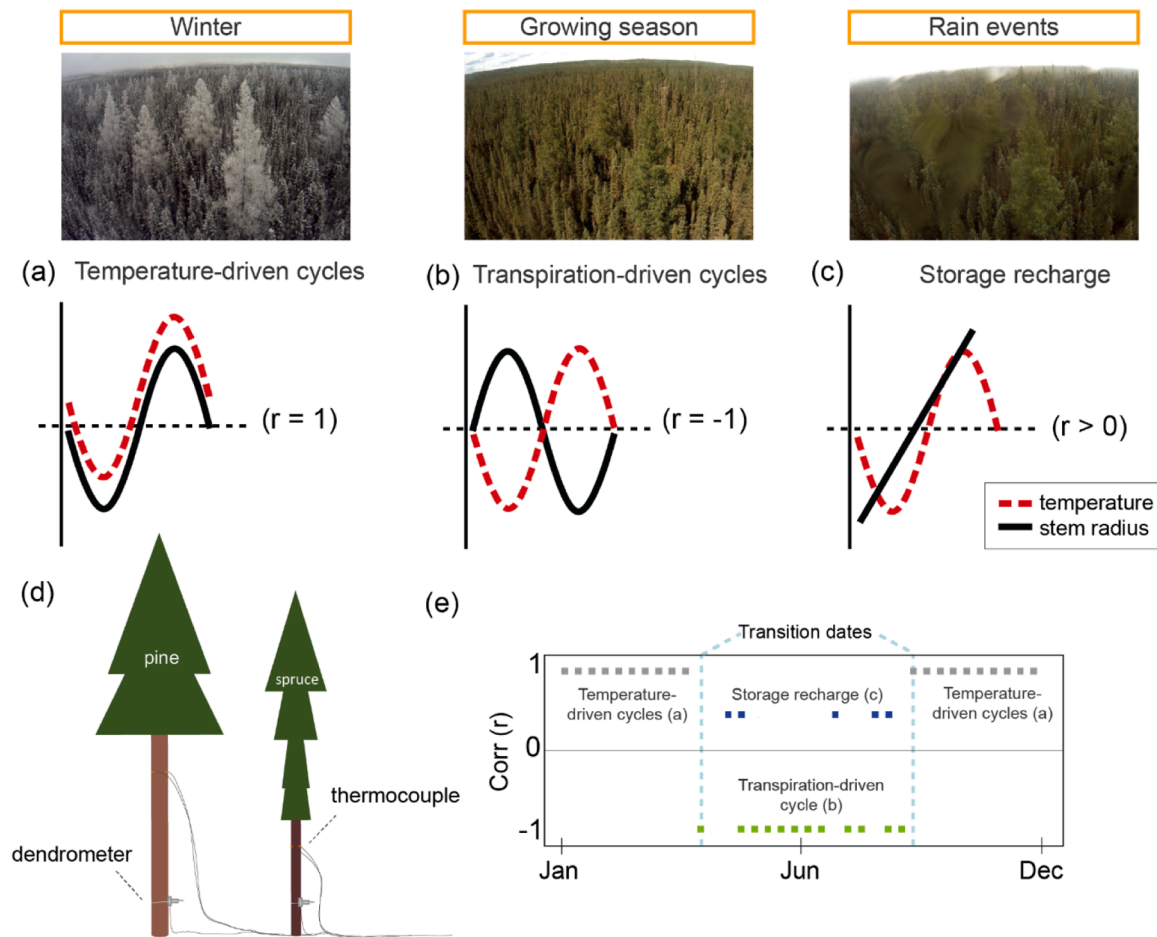
Fig. 1. Conceptual representation of the stem-temp approach. Panel (a) illustrates the temperature-driven cycle, typical in winter and early spring; this diurnal pattern leads to positive temperature-stem radius correlations ($r = 1$). Panel (b) shows transpiration-driven cycles and the inverse relationship of temperature and stem radius; this diurnal pattern leads to negative correlations ($r = -1$). Panel (c) radius change showing stem storage refilling resulting in stem expansion during early spring stem rehydration and/or after rainfall events during the growing season. Panel (d) illustrates field setting with dendrometer and thermocouples monitoring stem radius change and sapwood temperature, respectively. Panel (e) illustrates changes in the theoretical correlation coefficients throughout a typical year in the Boreal forest. Vegetation canopy pictures were downloaded from PhenoCam Network https://phenocam.sr.unh.edu/webcam/sites/canadaOBS/.

radius change is driven by a freeze-thaw cycle. Stems shrink due to low water potential gradients induced by ice formation in the xylem (Améglio et al., 2001; Zweifel and Hasler, 2001). Because the water potential over ice decreases 1.16 Mpa per 1° C decrease in ice temperature (Clausius–Clapeyron relationship; Guy, 1990; Rajashekar and Burke, 1982), a steep negative water potential generated by ice formation in the xylem drives the movement of unfrozen inner bark water towards the xylem ice with changes in temperature (Lintunen et al., 2017). Thus, during late fall and winter, stem radius changes follow the daily patterns in air temperature, with a minimum radius in the morning and a maximum radius in the afternoon. We use this understanding to develop the proposed approach.

2.1. The stem-radius-temperature correlation approach

The *stem-temp approach*, short version of stem radius-temperature correlation approach, leverages the stem diurnal cycle information and sapwood temperature to define phenological transition dates (Fig. 1). Because sapwood temperature is a direct measure of xylem conduit tissue temperature, and stem diurnal cycle a direct measure of the hydraulic signal, this information can be used to identify changes from temperature-driven cycle and to transpiration-driven cycles described above. The Pearson's correlation coefficient between diurnal stem radius change and sapwood temperature is positive when stem radius change is driven by temperature (i.e., tree hydraulic signal follows changes in air temperature, driven by the potential gradient generated by ice formation within the stem) (Fig. 1a), and negative during a transpiration-driven cycle (i.e., tree hydraulic shows opposite patterns to air temperature because stem diurnal cycle is driven by the potential gradient generated by transpiration) (Fig. 1b). When trees are refilling internal water storages after rainfall events and/or snowmelt, stem diurnal cycles show a continuous increase in stem radius, and a positive, but weak correlation coefficient (Fig. 1c).

The dynamic change in correlation coefficients between stem diurnal cycle and sapwood temperature indicates the phenological transition dates. The change from positive to negative correlation values in the spring indicates the end of the temperature-driven cycle (Fig. 1e). Thus, stem diurnal cycles no longer follows changes in air temperature. This is followed by the onset of stem rehydration (Fig. 1c) in the spring, which is defined by the shift from negative to positive correlation values ($r > 0$). The onset of rehydration shows a continuous increase in stem radius and weak, but positive, correlation coefficients. Stem rehydration is a key event in the boreal forest as trees refill internal water storage with the increase in moisture availability via snowmelt (Nehemy et al., 2022; Tardif et al., 2001; Young-Robertson et al., 2016). Following rehydration is the onset of transpiration with a shift from positive ($r > 0$; rehydration phase) to negative correlation values ($r < 0$; Fig. 1b). The negative correlation value continues throughout the growing season (Fig. 1e) with exception of rainy days when correlation values become positive ($r > 0$) (Fig. 1c, 1e). Later in the fall, the change from negative to

positive correlation ($r > 0$) values indicates the end of transpiration-driven cycles (Fig. 1e).

3. Material and methods

3.1. Site characteristics

The study was performed in two long-term research sites located at the southern edge of the Boreal Plains Ecozone in Saskatchewan, Canada. The sites are operated by the Boreal Ecosystem Research and Monitoring Sites (BERMS) program and were established by the Boreal Ecosystem and Atmosphere Study (BOREAS) program in 1993. The study interval comprises five years, from 2016 to 2020. The mean annual precipitation in the region is 517 mm, with a mean annual temperature of 1.7 °C (Prince Albert, Saskatchewan). The Old Black Spruce site (OBS) (53. 98 °N, 105.12 °W; AmeriFlux ID, CA-Obs) is a dense mixed forest stand dominated by black spruce with sparse (10% of stem density) eastern larch (*Larix laricina*) trees (Barr et al., 2012). The average black spruce height is 8.6 m and the larch is 11.9 m (Pappas et al., 2020). This forest stand is about 140 years old and was established after a forest fire. The soil is moderately to poorly drained, with a shallow peat layer that varies in depth across the site (10–20 cm). The Old Jack Pine site (OJP) (53. 92 °N, 104.69 °W; AmeriFlux ID, CA-Ojp) forest stand is composed of jack pine, with an average height of 15 m. The forest stand is approximately 100 years old and was also established after a forest fire. The soil is well-drained, loamy-sand soil. A more detailed description of the sites can be found at Maillet et al. (2022) and Pappas et al. (2020).

3.2. Stem radius: data collection and processing

We monitored stem radius changes of the dominant tree species at each site, black spruce and jack pine, using automatic circumference dendrometers (DC2 and DC3, Ecomatik, Dachau, Germany). Half-hourly stem radius measurements were recorded using HOBOUX120-006 M data loggers. A set of four dendrometers were connected to each data logger. The dendrometers monitored the stem radius of trees within the tower footprint of each site. The arrays were distributed near the tower and covered trees of different diameter and height. We monitored the stem radius change of 13 black spruce trees and 18 jack pine trees at breast height at OBS and OJP, respectively. The average stem diameter at breast height of monitored trees was 13 cm for black spruce and 17 cm for jack pine. We converted the raw recorded voltage measurements into a measure of radius change in μm according to manufacturer specification. More specifically, an R-script was developed based on the equation specific to this instrument provided by the manufacturer which converted our raw voltage measurements into a measure of radius change in relation to the diameter change of each individual tree (for specific equation see Ecomatik user manual; https://ecomatik.de/site/a ssets/files/13369/usermanual_dc3.pdf). We further processed the resulting data to eliminate any recording errors resulting from wildlife interfering in measurements by cutting wires, disturbing the instrument, or battery failure. We removed periods of data identified with such irregular measurements from specific sensors.

The stem diurnal cycles were computed following King et al. (2013). This data analysis provides information of the diurnal hydraulic related signal and was used in the stem-temp approach described below. The sub-hourly stem radius measurement ($SR_{<i}$) of each individual tree was averaged to hourly measurement, SR_i, where i indicates a specific hour of the day. After this step, the daily means for each tree was computed ($\overline{SR_t}$) [1] and subtracted from the hourly measurements to obtain the stem diurnal hydraulic related signal (SR_H) [2] according to King et al. (2013). Because of the synchronous variation in diurnal cycle between individuals of the same species, we report the average stem diurnal cycle from each species.

$$\overline{SR_t} = \frac{1}{n} \sum_{i=1}^{n} SR_i$$

$$SR_H = SR_i - \overline{SR_t} \tag{2}$$

We also report the sub-hourly stem radius in relation to its maximum radius recorded in the previous growing season according to Zweifel et al. (2016). We obtained the maximum stem radius from the previous growing season of each tree (SR_{max}) and subtracted it from the sub-hourly measurement of each specific tree ($SR_{<i}$) [3] We then obtained the species averaged SR. The stem radius value is negative until trees are able to refill internal water storages and initiate radial growth by surpassing the zero-growth line (Zweifel et al., 2016).

$$SR = SR_{<i} - SR_{max} \tag{3}$$

3.3. Tower based measurements: g_{cc}, ET, NEP, and $SIF_{relative}$

The vegetation 'greenness' index measured by the green chromatic coordinate (G_{cc}) was obtained from the PhenoCam Network (phenocam. unh.edu). This data was collected using a camera mounted at OBS tower of our study site and retrieves 30 min lapse images of the canopy. Each image is converted to a three-layer array that corresponds to the red, green and blue primary colours of the RGB spectrum. This information is used to calculate G_{CC} from a predefined region of interest (ROI) that represents the canopy of the studied tree species. Daily G_{CC} is obtained from the 90th percentile at 1-day intervals (Seyednasrollah et al., 2019; Sonnentag et al., 2012). We obtained the 'greenness rising' phenological transition dates of 10%, 25% and 50% and the 'greenness falling' of 50%, 25% and 10% of G_{CC} by using the LOESS-based method to smooth G_{CC} and define the seasonal amplitude (Richardson et al., 2018; Seyednasrollah et al., 2019). This indicates phenological transition dates of changes in canopy greenness in relation to G_{CC} seasonal amplitudes. For evergreen species, these transition dates indicate changes in the pigmentation at leaf level and are associated with changes photosynthetic capacity. We refer the reader to Richardson et al. (2018) and Seyednasrollah et al. (2019) for detailed information on image acquisition and data processing for G_{CC} at the sites. G_{CC} from phenocam images has been shown to track the onset of canopy level photosynthesis in spring and during cessation in the fall effectively (Seyednasrollah et al., 2021).

Eddy-covariance measurements of ET and net ecosystem production (NEP) were made at 29 m and 25 m above the ground at OJP and OBS, respectively. For all years at OJP and OBS starting in 2019, the eddy-covariance system consisted of a 3-D sonic anemometer (CSAT3, Campbell Scientific, Logan, UT) in combination with a closed-path infrared gas analyzer (LI-7200, Li-Cor Environmental, Lincoln, NE) for measuring H_2O and CO_2 fluctuations. The 30-min eddy fluxes were processed using the Eddy-Pro-software (version 7.0.6, Li-Cor Environmental, Lincoln, NE). At OBS from 2016 to 2018, the eddy-covariance system consisted of a 3-D sonic anemometer (model R3-50, Gill Instruments Ltd., Lymington, UK) in combination with a closed-path infrared (model LI7000, LI-COR Inc., Lincoln, NE, USA), enclosed in a temperature-controlled housing and operated in absolute mode. The 30-min fluxes were processed using the U.B.C. Biomet software. For further details, see (Kljun et al., 2006). A large gap in the flux data (ET and NEP) at OBS (25 Aug 2018 to 22 July 2019) remained unfilled.

We used measured NEP to identify the onset of net positive carbon uptake at the sites following (Ahmed et al., 2021), who showed that eddy-covariance measurements of NEP have a more distinct signature than ET of increasing canopy conductance in spring. Gap-filled NEP was integrated daily for each year and the cumulative value starting from January 1 was computed. The onset of carbon uptake occurs when cumulative NEP starts to continually increase in value in the spring (for exemplification, see Fig. 4 in Ahmed et al., 2021).

Solar-Induced Chlorophyll Fluorescence (SIF) measurements were made at OBS atop the site's 25 m tower using the spectrometer system PhotoSpec (Pierrat et al., 2022, 2021). PhotoSpec retrieved SIF in the

far-red (745–758 nm) wavelength range using a Fraunhofer line-based retrieval (Grossmann et al., 2018). This retrieval approach has a high signal-to-noise ratio so that the standard deviations of diurnal variability in the SIF signal are significantly higher than errors in SIF measurements (Grossmann et al., 2018; Pierrat et al., 2021). To account for illumination effects and a persistent winter light response of SIF (Pierrat et al., 2022), we calculated the relative SIF ($SIF_{relative}$) as $SIF_{relative} = SIF/I$, where I is the light intensity in the SIF retrieval window (Parazoo et al., 2020; Pierrat et al., 2021). PhotoSpec has a narrow field of view (FOV = $0.7°$) and a 2-D scanning capability, permitting independent SIF measurements for individual tree species (i.e., black spruce) $SIF_{relative}$ measurements were taken approximately every 20 s across a variety of vegetated targets. Here we report 30-minute averages of black spruce observations, which were then averaged again to report daily mean $SIF_{relative}$ and the standard deviation of the diurnal variability. Additional measurement details about the OBS site, including PhotoSpect set up can be found in Pierrat et al. (2021) and Pierrat et al. (2022), and further instrument details can be found in Grossmann et al. (2018).

3.4. Environmental variables

Air temperature was recorded using temperature/ humidity probes (model HMP45C, Vaisala Inc., Oy, Finland) above the canopy of the sites mounted in a radiation shield. Precipitation was recorded using an accumulating gauge (Geonor model T-200B all-weather weighing precipitation gauge with an Alter shield, GEONOR, Inc., Augusta, NJ, USA) located in a small forest clearing. Shallow soil temperature was also measured at both sites at 2 cm and 10 cm in two locations using a Type-T copper-constant thermocouples and averaged together. We use shallow soil temperature as an indication of ground surface temperature. Sapwood temperature was monitored using a Type-E chromel-constantan thermocouples inserted at 10 mm depth in the sapwood of the trees. The sensors were located at 12 m and 5 m in height at OJP and OBS, respectively. We had a south and north-facing sensor at each height that was then averaged for the overall analysis. All environmental data is recorded at 30 min time resolution.

Snow depth was continuously monitored at OJP and OBS using an ultrasonic snow depth gauge (UDG01, Campbell Scientific, Logan, UT, USA). Snow surveys were also conducted at each site once or twice per month between October and April. At OJP, a networked digital camera (P1357, Axis Communications, Lund, Sweden) mounted to the tower allows for visual canopy and snow ground cover monitoring through repeat photography at 30-min resolution. We used the snow depth measurements and visual ground cover information provided through images to determine the snowmelt period and the first snow free date at the sites.

3.5. Stem-temp approach and critical threshold

All data analysis and visualization were done in R (R Core Team, 2020). We first computed the average mean stem diurnal cycle for each species ($\overline{SR}_{sp}$) using the calculated $\overline{SR}_t$. Then, we computed the stem-temp approach by conducting a moving-window Pearson's correlation analysis (hourly resolution) between species' mean stem diurnal cycle ($\overline{SR}_{sp}$) and sapwood temperature, as well as air temperature (stem-air temperature approach). We used the package 'roll' (function roll_corr) (Foster, 2020). We defined statistically significant correlations at the 99% confidence (package: 'treeclim'; function [dcc], Zang and Biondi, 2015). We used the daily correlation value, which is the hourly correlation within the 24-hour window of the specific day in local standard time (r-value at the 24-hour period), to identify phenological transition dates in transpiration. Daily correlation values that surpass the critical correlation value for the two-tailed test at the 99% confidence level ($r = 0.515$; two-tailed) indicate then a statistically significant change in diurnal cycle patterns and identifies the phenological transition dates

described in Section 2.1 (Fig. 1).

3.6. Comparison between phenological approaches

We first defined the timing of phenological transition phases obtained from the stem-temp approach for black spruce and jack pine. We then compared phenological transition dates obtained from the stem-temp approach against the results obtained from the same approach when using air temperature. We calculated the difference between the transition dates (i.e., time lags in days) per year. We also computed the difference between stem-temp transition dates and G_{CC} ('greenness rising' and 'greenness failing') and the NEP-based phenological transition dates. We evaluated the agreement between the transition dates obtained from these different phenological approaches using a Pearson's correlation analysis. We visually compared the stem-temp transpiration transition dates with ET and SIF data. We further compared the assessment of transpiration phenology with another important phenological event in the boreal forest - the snowmelt. We defined the snowmelt period based on observations of decrease in snowpack depth and ground surface temperature (Zhang, 2005).

4. Results

4.1. Stem-temp approach: phenological assessment of transpiration

The stem-temp approach provided useful information on the timing of transpiration phenological changes (Fig. 2). Fig. 2 shows the daily correlation values between diurnal stem cycles and sapwood temperature – the index of this approach (Fig. 2d). The changes in daily correlation indicated (i) the end of temperature-driven cycles, (ii) onset of rehydration and (iii) onset of transpiration-driven cycles in the spring, and (iv) the end of transpiration-driven cycles in the fall. Here we show only 2018 data for jack pine at OJP site. The method was applied to all years and species (see Supplementary Information for 2016, 2017, 2019 and 2020; Figures S1 to S7). Below we describe transpiration phenology phases and the proposed approach in detail.

4.1.1. Transpiration phenology in four phases

The first phase change in transpiration phenology was the (i) end of temperature-driven cycles characterized by an abrupt change in correlation value from positive to negative that surpassed the critical threshold value ($r = -0.515$) and that was statistically significant (Fig. 2d). The change in correlation was in agreement with statistical assessment of significance. In this phase, stem radius showed a decrease in stem size (Figure 2a; DOY 105 and 106) and did not follow changes in air temperature. The end of temperature-driven cycles (Fig. 2a) was characterized by a maximum amplitude in stem radius and positive sapwood temperatures in the morning. Following the negative correlations between stem radius and sapwood temperature (Fig. 2c,d), we observed the second phase change in transpiration phenology characterized by the (ii) onset of stem rehydration. Rehydration characterizes by a short interval with positive, but weak correlation values (Fig. 2c,d) with continuous stem swelling (Fig. 2a; DOY 108 −114) and an abrupt increase in stem radius (Fig. 2e).

Following a short period of stem rehydration, the third phase change in transpiration phenology characterizes the (iii) onset of transpiration. The onset of transpiration and shift to transpiration-driven cycles was characterized by the change from positive to negative correlation value that surpassed correlation threshold values (Fig. 2c; DOY 115). This shift was also observed with a characteristic transpiration-driven cycle, with a maximum stem radius in the morning, and minimum in the afternoon (Fig. 2a; DOY 115). The onset chracterizes the change to negative correlation values that surpasses the threshold for at least two days ($r = -0.515$). After the onset of transpiration, we observed a continuous negative correlation value throughout the growing season (Fig. 2c,d), with exceptions on rainy days (Fig. 2d).
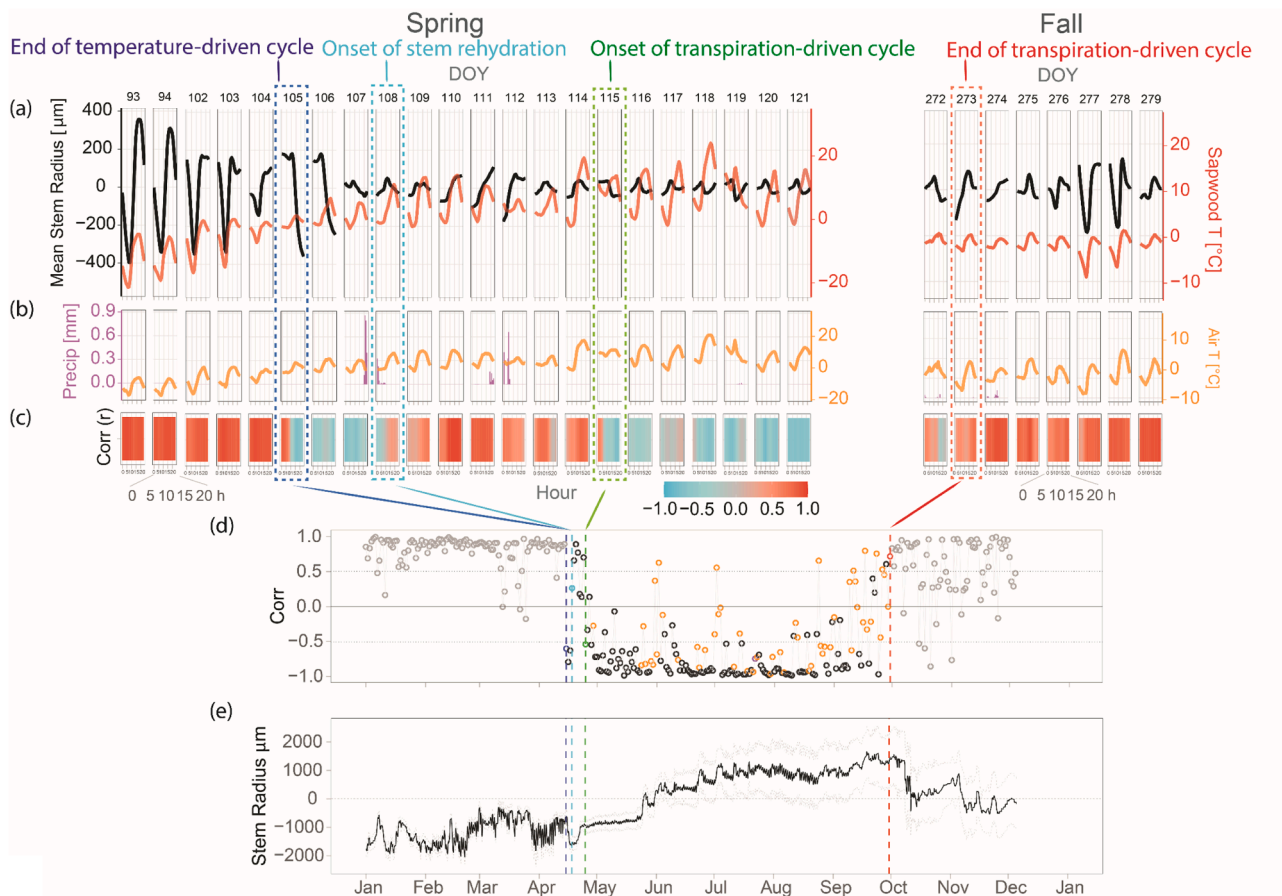
Fig. 2. Phenological assessment of transpiration using the stem-temp approach. The figure displays 2018 data from jack pine. Panel a) shows Mean Stem Radius (i.e., mean diurnal cycles; black lines) following King et al. (2013), along with sapwood temperature (red) from April 3 to May 6 (DOY 93 to 121) and September 7 to October 11 (DOY 272 to 279), respectively. Panel b) shows precipitation (Precip; purple) and air temperature (Air T; yellow) during the same time interval as respective above panels. Panel c) shows moving hourly correlation analysis between stem radius and sapwood temperature for the same period as the above panels. Panel d) shows daily correlation values between stem radius and sapwood temperature throughout the year; orange dots indicate days with precipitation events between later morning and early afternoon. Panel e) shows stem radius change in relation to previous' year maximum radius (Zweifel et al., 2016) (zero-line) and dashed lines region shows the standard deviation for the 30 min time resolution measurement.

The fourth and final phase occurred later in the growing season (Fig. 2a). This was characterized by the (iv) end of transpiration-driven cycles which was indicated by a statistically significant change to positive correlation surpassing the critical threshold value; followed by continuous positive correlations, and at least one day above the threshold ($r = 0.515$) (Fig. 2c). During this period, we also observed a maximum amplitude in stem radius in the afternoon, and later a clear temperature-driven cycle (e.g., Fig. 2; Fall). This phase also overlapped

with the decrease in air temperature and sapwood temperature below 0 ℃ during daytime and nighttime.

4.2. Phenological assessment of transpiration in evergreen species and distinct study sites

Black spruce and jack pine spring phenological transition dates were strikingly synchronous during the five year monitoring period (Fig. 3).
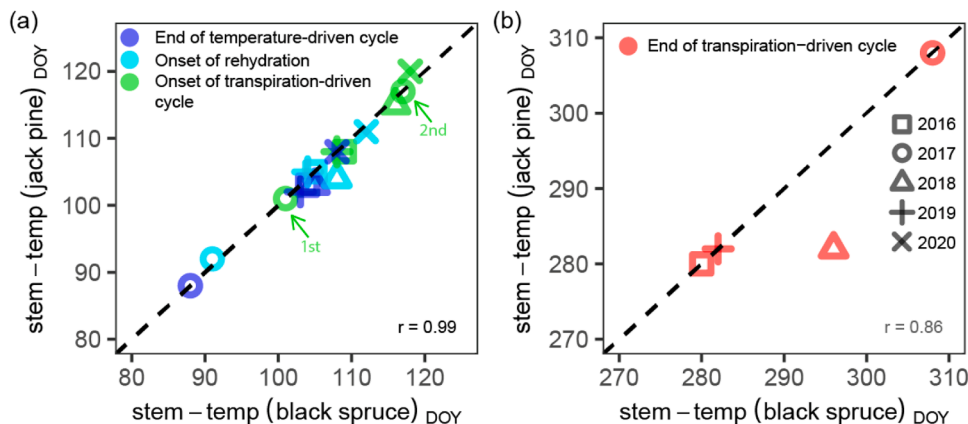

Fig. 3. Comparison of black spruce transpiration phenology transition dates with jack pine (DOY = day of year). Both species transition dates were obtained using the stem-temp approach. Panel a) shows spring transition phases and correlation value (r) between jack pine and black spruce ($p < 0.05$). Panel d) shows fall transition phase and correlation value between jack pine and black spruce ($p > 0.05$). The dashed line is the 1:1 line. Arrows in panel a) indicate first (1st) and second (2nd) onset of transpiration in 2017.

We observed a high correlation ($r = 0.99$; $p < 0.05$) between transition dates in the spring (Fig. 3a). The mean difference on the timing was less than 1 d for all spring phases: (i) end of temperature-driven cycles in the spring, (ii) onset of stem and (iii) onset of transpiration-driven cycles (Table 1). In 2017, there were two onsets of transpiration (Fig. 3a). We report the means (Table 1) in relation to latest onset because of the continuous transpiration-driven cycle (Fig. 1b) indicating the onset of the growing season.

We also observed periods of freezing in some springs. In 2017, there was an early end of temperature-driven cycle (DOY 88; Figs. S2 and S3), followed by an early onset of rehydration on DOY 91 for black spruce, and one day later for jack pine (DOY 92) in comparison with the other years (Table 1). Both species also showed a much earlier onset of transpiration, on DOY 101 (Fig. 3a). However, a long-freezing period with snowfall and drop in air temperature, resulted in the drop of sapwood temperature below 0 ℃, and end of transpiration-driven cycle (Figs. S2 and S3). Both species showed a final onset of transpiration, with continuous transpiration-driven cycle, after this long freezing period, on DOY 117 (Fig. 3a). In 2019, a shorter refreezing period resulted in a temporary cessation of the transpiration-driven cycles after the onset (Figs. 4 and 5). There was a drop in air temperature below 0 ℃ at night, with decrease in average daily air temperature, and precipitation fell as snow during this interval. Stem diurnal cycle and correlation analysis indicated that trees were not transpiring.

The two species behaved similarly in the fall (Fig. 3b). The end of transpiration-driven cycles occurred on DOY 291.5 ± 11.3 d for black spruce and jack pine on DOY 285.7 ± 13.2 d (Table 1). The correlation between the transition dates in the fall was lower than in the spring and was not statistically significant ($r = 0.86$; $p > 0.05$). The species behaved in unison, except in 2018. In 2018, while the stem-temp approach showed a clear transition phase for jack pine on DOY 273 (Fig. S5), black spruce transition was not clear (Figure S4). Black spruce showed variability between positive and negative correlation values, until a clear transition phase on DOY 296. In the fall of 2018 during the transition period for both species, air temperature dropped below 0 ℃ but returned to positive air temperatures. The oscillation in air temperature might have resulted in the observed differences between species, or the failure of the method.

4.3. Method comparison: sapwood temperature and air temperature

The stem-temp approach between stem radius and sapwood temperature versus stem radius and air temperature indicated similar phenological timing for black spruce and jack pine (Table 1). We observed no difference when using sapwood temperature or air temperature when detecting the end of temperature-driven cycles for black spruce across the observed period (Table 1). However, in 2016 and 2019 correlations between air temperature and black spruce stem radius did not surpass the critical threshold and failed to indicate the end of temperature-driven cycles (Fig. S8 d). Jack pine showed a small offset on the end of temperature-driven cycles in the spring when comparing air temperature and sapwood temperature (Table 1). Onset of stem rehydration showed no difference when using sapwood temperature or air temperature for black spruce and for jack pine. The stem-temp approach using air temperature failed to detect the end of the temperature-driven cycle and onset of rehydration in 2020 for jack pine. The onset of transpiration detected by sapwood and air temperature were offset by 2.6 and 3.6 d for black spruce and jack pine, respectively when compared with stem-temp using sapwood temperature. The timing for end of transpiration-driven cycles in the fall was showed larger differences between methods (Table 1).

4.4. Transpiration transition dates relationship with GCC, cumulative NEP, SIF$_{relative}$, ET, and environmental conditions

The transition dates in the spring obtained from the stem-temp approach and the GCC were aligned and strongly correlated ($r = 0.82$; $p < 0.05$) (Fig. 7a). Our data showed that the end of temperature-driven cycles aligns well with the 10% transition phase ('greenness rising') of G$_{cc}$ at OBS (Fig. 7). The end of the freeze-thaw cycle was observed 3.6 d after the 10% greenness rising within all five observed years (Table 1). The onset of transpiration occurred approximately at the same time as the 25% transition in G$_{cc}$ for black spruce (Fig. 7a) with an average offset of 1 d (Table 1) which is within observed uncertainty for G$_{cc}$ (8 d; $n = 5$). The end of transpiration-driven cycle also showed a good agreement with G$_{cc}$ fall transition dates ('greenness falling') ($r = 0.99$; $p < 0.05$). On average end of transpiration-driven cycles occurred −0.5 d before the 10% Gcc falling transition phase (Fig. 7b; Table 1). In 2019 (Fig. 4e) and 2016 (Fig. 6c) and the end of transpiration-driven cycle was closer to the Gcc 25% 'greenness falling' rather than the 10%, and it was observed in both years.

The onset of transpiration observed with the stem-temp approach was strongly correlated with the transition date for the onset of carbon uptake observed with cumulative NEP at both sites (Fig. 7c and d). Black spruce onset of transpiration was 2 d earlier and jack pine −0.8 d later than the onset of carbon uptake at the site for the five-year observation (Table 1).

The timing of end of temperature-driven cycles and onset of transpiration in the spring are also aligned with observed increase in ET at both sites in 2019 (Figs. 4 and 5) and other years (Fig. 6; Figs. S1 to S7).

Table 1

Comparison between the stem-temp approach transition dates for the four phenological phases between jack pine and black spruce and comparison between stem-temp approach transition dates with other phenological approaches. Transitions date: mean transition date (DOY; day of the year) and SD shows the standard deviation. Mean difference: The mean difference obtained between transition dates (i.e., lag in days) obtained between compared methods or species. Stem-temp (air temperature) indicates the use of air temperature instead of sapwood temperature. OBS: Old Black Spruce site; OJP: Old Jack Pine site.

|	Site	Phenological method	End of temperature-driven cycle		Onset of rehydration		Onset of transpiration		End of transpiration-driven cycle	
			DOY	SD	DOY	SD	DOY	SD	DOY	SD
Transition date (Mean ± SD)	OBS	stem-temp	101.6	7.0	104.00	7.1	113.6	5.6	291.5	11.3
Transition date	OJP	stem-temp	101.2	6.9	104.20	6.5	113.6	4.8	285.75	13.3
Mean difference	OBS-OJP	black spruce vs. jack pine	0.4	0.5	−0.2	0.7	0.0	1.1	5.7	10.0
Transition date	OBS	stem-temp (air temperature)	100.3	8.8	103.7	9.1	116.2	6.4	285.2	9.8
Transition date	OJP	stem-temp	99.7	5.7	102.5	14.8	102.5	14.8	291.7	16.5
Mean difference	OBS	stem-temp vs. stem-temp (air)	0.0	0.0	0.0	0.0	−2.6	2.8	6.2	11.2
Mean difference	OJP	stem-temp vs. stem-temp (air)	−0.2	0.4	0.0	0.7	−3.6	2.1	−6.00	12.3
Transition date	OBS	Greenness index (Gcc)	98.0	7.7			112.6	3.61	292.0	7.7
Mean difference	OBS	Gcc vs. stem-temp	3.6	2.7			1.0	1.3	−0.5	3.8
Transition date	OBS	cumulative NEP					114.5	3.9		
Transition date	OJP	cumulative NEP					114.6	5.3		
Mean difference	OBS	cumulative NEP vs. stem-temp					0.5	0.9		
Mean difference	OJP	cumulative NEP vs. stem-temp					−1.0	1.7		
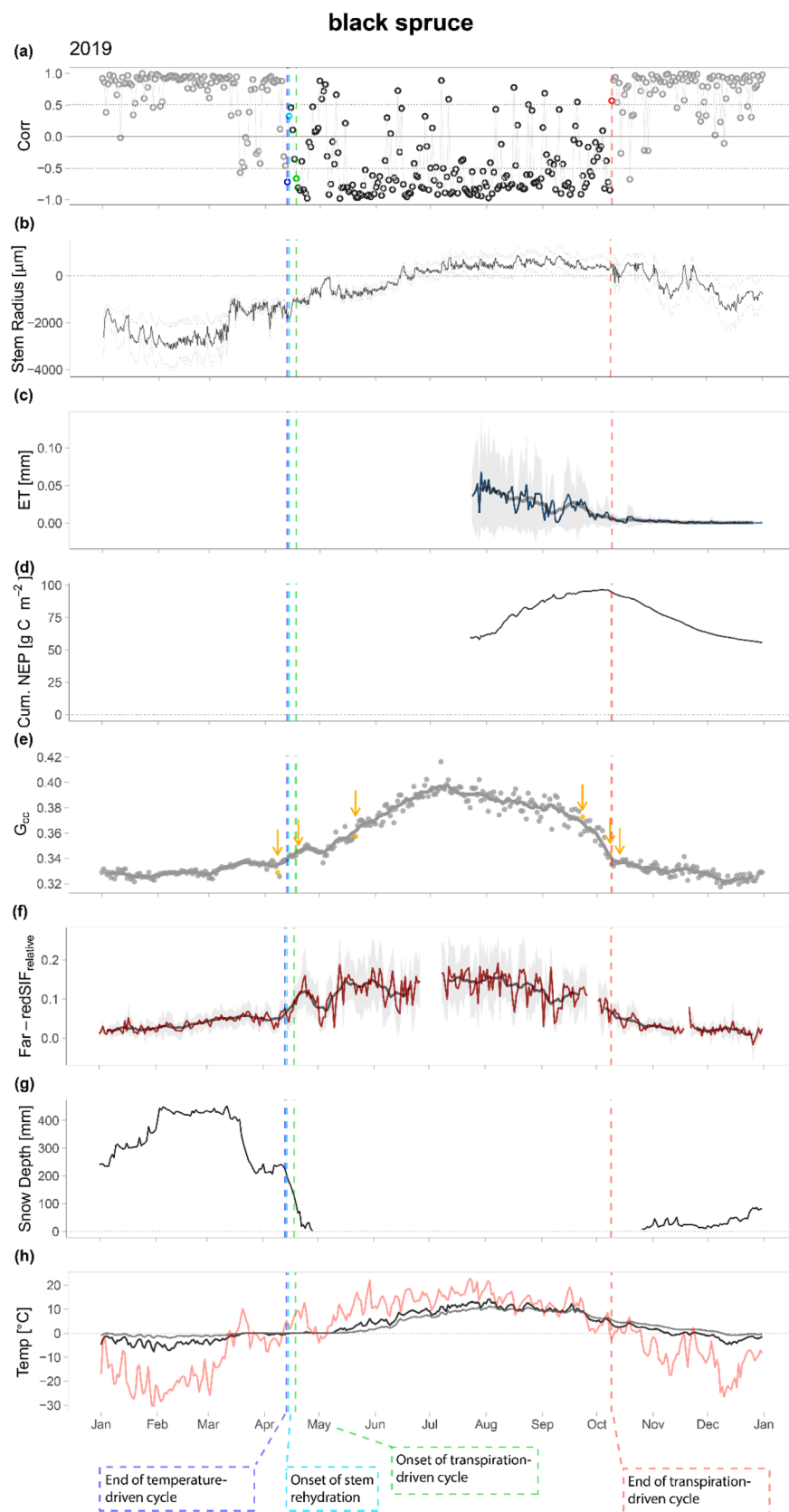
Fig. 4. Old Black Spruce site data collected in 2019 showing timing of transpiration phenological phases for black spruce in the spring and fall. Panel a) shows daily correlation values between stem radius and sapwood temperature throughout the year. Panel b) shows stem radius change in relation to zero-growth line (zero line; previous' year maximum radius (Zweifel et al., 2016)) and dashed lines region shows the standard deviation for the 30 min time resolution measurement. Panels c) shows daily average evapotranspiration (ET) and the standard deviation in shaded gray. Panel d) shows cumulative net ecosystem production (NEP) indicating the onset of carbon uptake by red arrow. Panel e) shows Gcc and yellow dots indicate transition phases in sequence, 10% rising transition, 25% rising transition, 50% rising transition, 50% falling transition, 25% falling transition, 10% falling transition (with arrows). Panel f) shows daily averaged SIF relative data. Panel g) shows snow depth. Panel h) shows shallow soil temperature (2 and 10 cm) and air temperature. Figures showing other years can be found in the Supplementary Information (FigureS1 to S7).
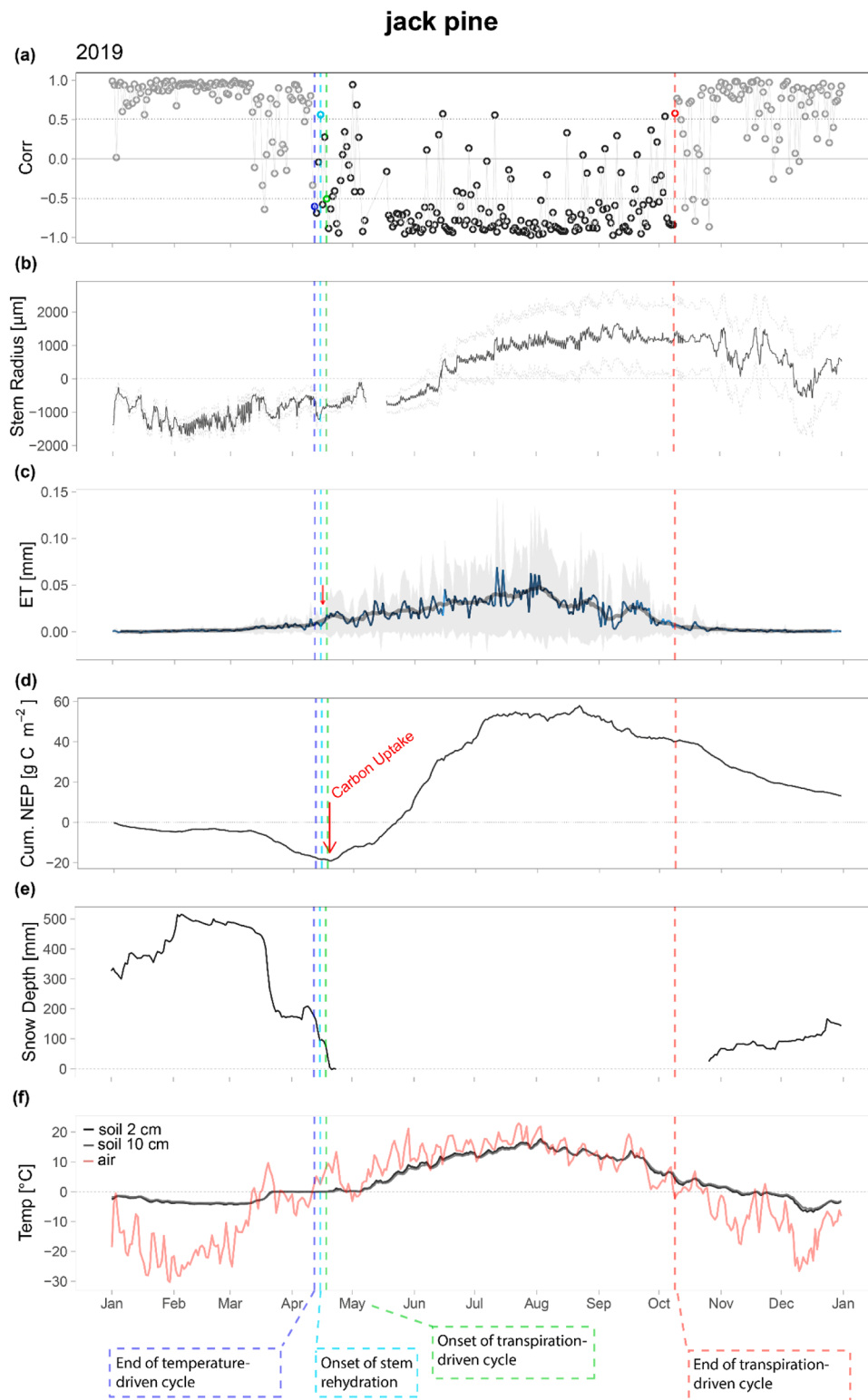
Fig. 5. Old Jack Pine site data collected in 2019 showing timing of transpiration phenological phases for jack pine in the spring and fall. Panel a) shows daily correlation values between stem radius and sapwood temperature throughout the year. Panel b) shows stem radius change in relation to zero-growth line (zero line; previous' year maximum radius (Zweifel et al., 2016)) and dashed lines region shows the standard deviation for the 30 min time resolution measurement. Panels c) shows daily average evapotranspiration (ET) and shaded are the standard deviation. Small red arrows indicate small decline in ET after onset of rehydration. Panel d) shows cumulative net ecosystem production (NEP) indicating the onset of carbon uptake by red arrow. Panel e) shows snow depth. Panel f) shows shallow soil temperature (2 and 10 cm) and air temperature. Figures showing other years can be found in the Supplementary Information (Figs. S1 to S7).

$SIF_{relative}$ in 2019 for black spruce aligned with the end of temperature-driven cycles and the onset of transpiration (Fig. 4e). We observe an initial peak in $SIF_{relative}$ during the end of the freeze-thaw cycle, followed by a small decline during stem rehydration, and a second peak in $SIF_{relative}$ is observed during the onset of transpiration. The decline in ET in the fall is also in agreement with the end of the transpiration-driven cycles in the fall at both sites (Figs. 4c, 5c and 6c). The days with sporadic transpiration observed in 2019 after the end of transpiration-driven cycles in the October indicated by the negative correlations that surpass critical thresholds, aligns with a small peak in ET at both sites and $SIF_{relative}$ at OBS (Figs. 4a,c and 5c).

The onset of transpiration overlapped with snowmelt in both sites throughout the observed period (2016–2020) (Figs. 4g, 5e and 6f; Figs. S1 to S7). OBS and OJP snowmelt end date (i.e., date with no snow on the ground) occurred on DOY 122.6 ± 5.0 and 120 ± 5.1, respectively (*n* = 5). The onset of transpiration occurred during the main melt
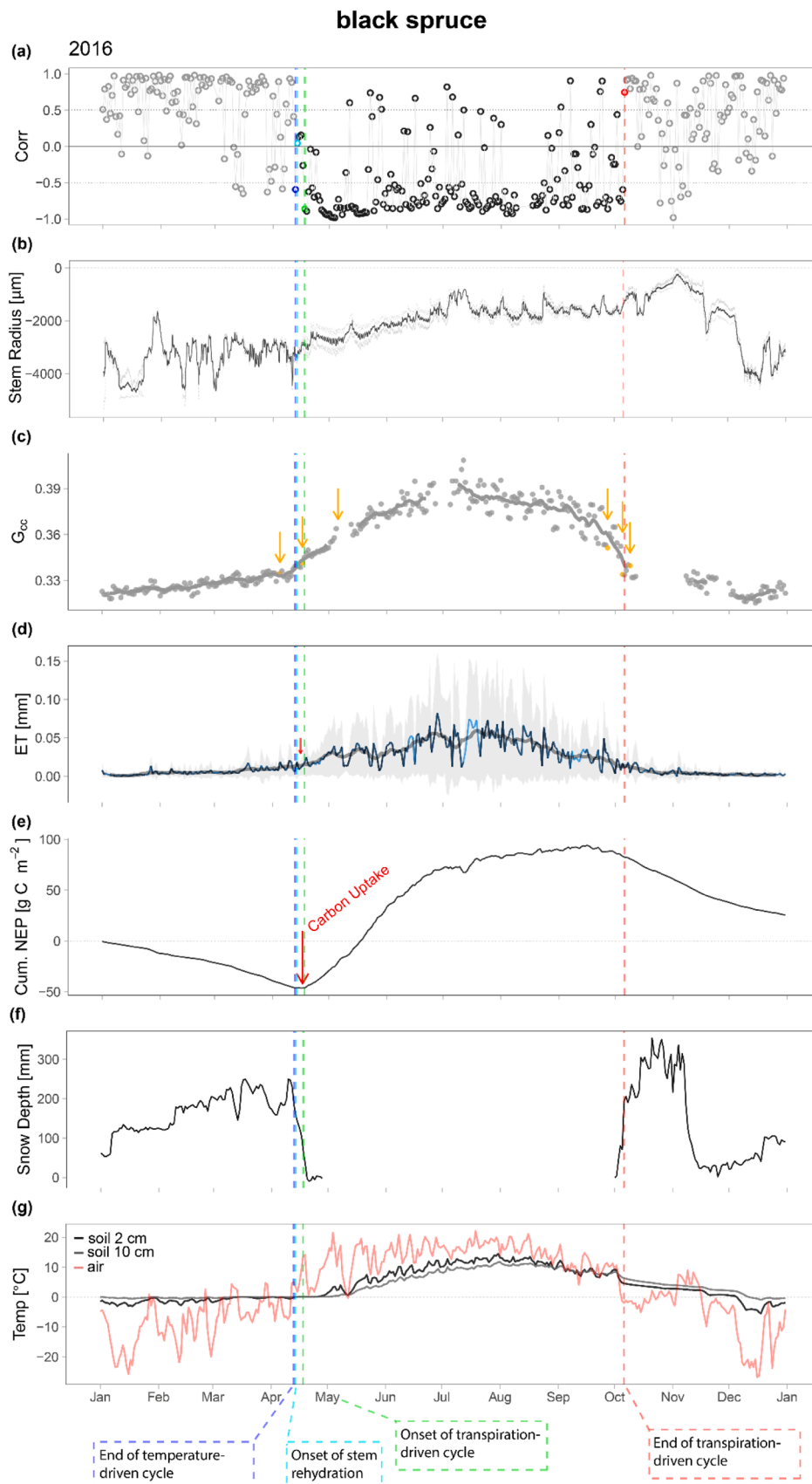
Fig. 6. Old Black Spruce site data collected in 2016 showing timing of transpiration phenological phases for black spruce in the spring and fall. Panel a) shows daily correlation values between stem radius and sapwood temperature throughout the year. Panel b) shows stem radius change in relation to zero-growth line (zero line; previous' year maximum radius (Zweifel et al., 2016)) and dashed lines region shows the standard deviation for the 30 min time resolution measurement. Panels c) shows daily average evapotranspiration (ET) and shaded are the standard deviation. Small red arrows indicate small decline in ET after onset of rehydration. Panel d) shows cumulative net ecosystem production (NEP) indicating the onset of carbon uptake by red arrow. Panel e) shows Gcc and yellow dots indicate transition phases in sequence, 10% raising transition, 25% raising transition, 50% raising transition, 50% falling transition, 25% falling transition, 10% falling transition. Panel f) shows snow depth. Panel g) shows shallow soil temperature (2 and 10 cm) and air temperature. Figures showing other years can be found in the Supplementary Information (Figs. S1 to S7).
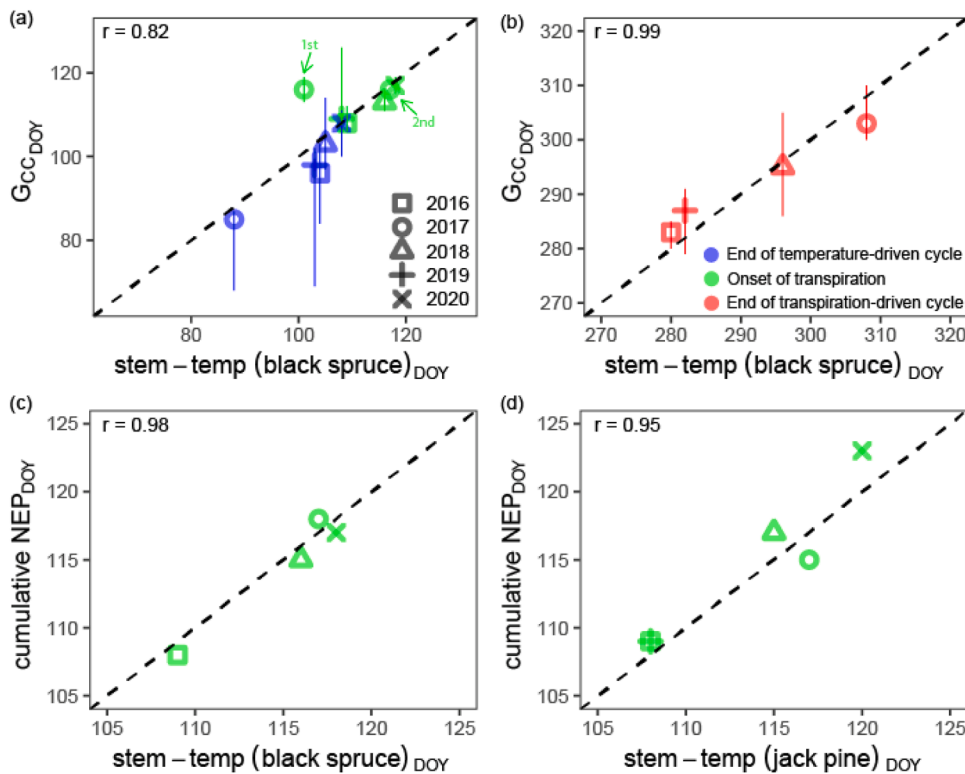
Fig. 7. Comparison of spring and fall vegetation phenological transition dates determined by the stem-temp approach with 'greenness rising' (a) and 'greenness falling' (b) from green chromatic coordinate (G_{cc}) and onset of carbon uptake from cumulative NEP. Panel a) shows the end of freeze-thaw cycle transition is directly compared with the 10% rising transition (G_{cc}), and the onset of transpiration transition with the 25% rising transition (G_{cc}), in the spring. Arrows in panel a) indicate first (1st) and second (2nd) onset of transpiration in 2017. Panel b) shows the end of transpiration-driven cycle is compared with the 10% falling transition in the fall. The significant correlation ($p < 0.05$) values (r) are indicated in each subplot. G_{CC} uncertainties are shown as error bars. The dashed line is the 1:1 line.

period and before the end of the main snowmelt for both black spruce and jack pine. The end of transpiration-driven cycles was not directly associated with snowfall timing. For example, the end of transpiration-driven cycle 2019 occurred before accumulation of snow on the ground (Figs. 4g and 5e), but after in the other years (Figs. S1 to S7).

5. Discussion

Vegetation phenology drives the seasonality of carbon and water cycles (Keenan et al., 2014; Richardson et al., 2013; Wolf et al., 2016). While a wide-range of metrics are available to monitor canopy-level phenological changes related to photosynthetic activities (e.g., G_{CC}, SIF, CCI), there is no alternative metric to evaluate transpiration phenology in the boreal forest. Our work here shows that the stem-temp approach using stem diurnal cycles and sapwood temperature is useful in describing phenological transition dates .

5.1. How does the stem-temp transition dates compare between species and to other approaches?

Our stem-temp approach allowed us to observe the timing of phenological changes in transpiration and characterize four transition phases (i) the *end of temperature-driven cycle*, (ii) the *onset of stem rehydration* and (iii) the *onset of transpiration* in the spring, and (iv) the *end of transpiration-driven cycles* during the end of the growing season in the fall. This method provides high-temporal resolution assessment of phenological transition dates in transpiration that have not been previously reported in the literature. The stem-temp approach diverges from previous seasonal assessments of stem radius change (Tardif et al., 2001; Turcotte et al., 2009) because it allows daily assessment of the timing of transpiration phenological changes with a focus on tree hydraulics instead of radial growth. Additionally, the stem-temp approach does not depend on knowledge of species-specific sap freezing point to define phenological transition dates; nor does it need weeks of data for statistical assessment of transition dates because it evaluates the change in correlation using daily stem cycle and sapwood temperature. While it

has been difficult previously to identify rehydration and onset of transpiration in cold environments (Kozlowski and Winget, 1964; Mäkinen et al., 2008; Tardif et al., 2001) the proposed approach provides mechanistic assessment that uses physiological knowledge and goes beyond graphical analysis.

The stem-temp approach builds directly on research that provides physiological understanding of the phenomena (Améglio et al., 2001; Sevanto et al., 2006; Steppe et al., 2006; Zweifel and Häsler, 2000). The diurnal change in stem radius is closely related to changes in water potential gradients between xylem and inner bark. In the warm months of the year, transpiration is the driver of shrinkage and expansion of the inner bark; whereas in colder months air temperature is the driver (Zweifel and Häsler, 2000). We tested the approach across two coniferous species growing at different sites from 2016 to 2020. Our data showed that the proposed approach was able to track transpiration phenology in both species. However, the approach might be limited to evergreen species, and future investigation is necessary across different species and growing forms.

Black spruce and jack pine showed close timing of phenological transition dates, with a maximum offset of only one day observed between them. Both evergreen species' aligned timing of transpiration onset in the spring and fall senescence could result from their site proximity (approx. 40 km) and similar local environmental conditions. A previous study showed that the reactivation of photosynthesis and transpiration in evergreen species in the spring is mainly driven by increased air, soil temperature, and soil water content (Pierrat et al., 2021). In the boreal forest, the increase in soil water content in the spring occurs via snowmelt. A 15 years investigation showed that spring snowmelt start date and soil thaw at OBS and OJP sites occurred on the same day (Ahmed et al., 2021). This synchronous increase in moisture availability and soil thaw at both sites might explain the strong correlation and close phenological transpiration transition dates observed between species in our study (Fig. 3). The aligned onset of transpiration between sites is also consistent with previous observations of similar onset dates for carbon uptake between sites, with a mean difference of 3 days (2001–2015) (Ahmed et al., 2021). The onset of transpiration in the

spring was consistent at the end of April, with a small variability on this date within a five-year observation period (Table 1). However, there was larger variability in the fall transition date for the end of transpiration-driven cycles compared to the onset of transpiration (Table 1). The end of transpiration driven cycles was observed between late September and early November. Thus, the length of the active transpiration season seems to be more impacted by the timing of fall transition phase rather than spring onset at the studied sites. This opens new opportunities for further investigation of fall vegetation phenology as this has been less studied than spring phenology (Montgomery et al., 2020) and could explain interannual variability of NEP (Wu et al., 2013). To the best of our knowledge, this is the first assessment that shows autumn transpiration phenology.

Overall phenological transition dates obtained from the stem-temp approach using sapwood temperature and air temperature were in good agreement. Sapwood temperature showed stronger correlations to stem diurnal cycle and might be preferred when using this approach in comparison to air temperature. The later showed weaker correlation with stem radius that may not surpass the critical threshold for statistical significance. This explains some of the offset between approaches, when using sapwood temperature versus air temperature. Beyond the stem-temp approach, we explored a phase-shift analysis which considers only the phase shift of the circadian cycle. A more detailed explanation and assessment can be found in the Supplementary Information (Session 2, Figs. S8 and S9).

Our transpiration phenological transition dates obtained with the stem-temp approach were compared with canopy-level eddy-covariance derived ET and NEP, remotely sensed products, and measurements of environmental conditions (i.e., snow cover, air temperature and soil temperature). While these measurements represent distinct processes (i.e., transpiration, evapotranspiration, photosynthetic activity and carbon uptake) and at different scales (i.e., ecosystem and tree level), the underlying physiological processes are intrinsically related, as shown by previous studies in evergreen forests (Bowling et al., 2018; Pierrat et al., 2021; Sevanto et al., 2006). Additionally, previous vegetation phenology investigations comparing different methods, such as canopy-level eddy covariance measurements (i.e., the onset of carbon uptake), repeated photography from canopy (i.e., G_{cc}) and ground observations of budburst showed strong agreement when detecting phenological transition dates at different spatial scales (Richardson et al., 2018; Seyednasrollah et al., 2021).

Here, we show that field-based transpiration phenological assessment using stem radius monitored within the tower footprint (Chen et al., 2012, 2011) aligned well and showed a strong correlation with the transition date of onset of net positive carbon uptake observed with cumulative NEP at both sites. On average, the mean difference between the onset of transpiration and carbon uptake at OJP and OBS was equal to, or smaller by one day, respectively (Table 1). This also supports previous work that showed a strong temporal correlation between tree-level stem radius change and tower-based NEP measurements in an evergreen forest (Zweifel et al., 2010). We also observe increased evapotranspiration at both sites during the onset of transpiration, but where the onset of ET is less clear. Small peaks in ET during the spring align with the end of temperature-driven cycles and onset of transpiration, showing a small decline in ET during stem rehydration (Figs. 5 and 6). Additionally, our proposed method allows observations of transpiration during sporadic warm days after the end of the transpiration-driven cycles. For example, we observed a single day or few days where correlation coefficients surpassed the negative threshold indicating transpiration after the end of the growing season in 2016 (Fig. S1), 2018 (Fig. S5) (at OJP only) and 2019 (Figs. 4 and 5). This occurred on days when air temperature (but not necessarily soil temperature) briefly rose above 0 °C. These days aligned with small peaks in ET. The analysis offers a novel approach for understanding the potential for wintertime photosynthetic activity (Sevanto et al., 2006) which is projected to increase under future climate warming scenarios (Vitasse

et al., 2018).

We compared the timing of transpiration phenological changes with remotely sensed G_{cc} and $SIF_{relative}$ to explore the link between stem radius measurements and canopy-level phenological change. The data showed s strong correlation between the stem-temp and G_{cc} phenological transition dates (Fig. 7) .The end of temperature-drive cycles is in good agreement with the 10% 'greenness rising' transition date, and that the onset of transpiration indicates a great coherence with 25% 'greenness rising' transition dates from G_{cc}. The end of transpiration-driven cycles in the fall was observed near the 10% and 25% 'greenness falling' transition dates. Furthermore, the end of temperature-driven cycle, onset of transpiration in spring and the end of transpiration-driven cycle in fall align closely with variability in $SIF_{relative}$. Additionally, changes in transpiration-driven cycles are reflected in $SIF_{relative}$ and G_{cc} signals. In particular, in 2017 and 2019, we observed the onset of stem rehydration and transpiration that was followed by a period of no transpiration-driven cycles and a corresponding decrease in $SIF_{relative}$ (in 2019) and G_{cc} signals. After slightly more than a week, trees resumed transpiration and we observed increases in both G_{cc} and $SIF_{relative}$ signals. These relationships are explored further in Pierrat et al. (2021). $SIF_{relative}$ has been shown to effectively track seasonal changes in photosynthetic phenology (Magney et al., 2019; Parazoo et al., 2018; Pierrat et al., 2021, 2022) as well as having generally good agreement with G_{cc} (e.g., Melaas et al., 2016; Richardson et al., 2018; Seyednasrollah et al., 2020). Thus, transpiration phenological assessment that focus on the timing of changes in tree hydraulics and stem temperature are well aligned with canopy-level observations that reflect photosynthetic activity. The comparison across methods that provide insights into distinct, but interrelated processes (i.e., transpiration and photosynthetic activity) highlights the advantage of combining distinct approaches to study vegetation phenology.

Finally, phenological assessment using stem-radius and sapwood temperature measurements provides a unique opportunity to investigate species-specific phenological responses to environmental change beyond what eddy-covariance derived measurements can provide alone. Eddy-covariance derived ET are spatially integrated and influenced by understory activity and evaporation (Chu et al., 2021; Pappas et al., 2020). The stem-radius measurements are species-specific and provide viable measurements under variable terrain and weather conditions. Thus, stem-temp approach enables phenological assessments of transpiration only and can complement eddy-covariance measurements. The combination of stem-temp approach and eddy-covariance method allow comparison of onset of transpiration, evapotranspiration, photosynthetic activity, and carbon uptake at the stand level as shown here (Figs. 4 to 6) and allows investigation of the synchronicity of these distinct processes. This evidence the usefulness of this alternative approach in tracking phenological transition dates in the boreal forest. Additional investigation is needed to understand how the results presented here compare to other evergreen sites.

The stem-temp approach is extremely useful during periods where snow cover may obscure remote sensing observations from both satellite or tower-based measurements (Pierrat et al., 2022, 2021). Even Gcc, which is simple and proven useful phenological measurement is disturbed by snow cover. There are periods during the transition phase where snow intercepted by the canopy does not allow continuous Gcc monitoring as we observed at OBS. The higher snow-catch efficiency of the jack pine canopy when compared to black spruce did not allow assessment of Gcc transition dates at this site. We observed more days with snow cover from canopy images at OJP (phenocam.nau.edu/-webcam/sites/canadaojp/) when compared to OBS, which may be related to the difference in branch and foliage architecture (i.e., jack pine has longer and stiffer needles that grows in bundles, with branches growing laterally or ascending). The higher snow-catch efficiency of individual jack pine trees (i.e., not rereferring to stand density of the site, but individual level) when compared to black spruce trees have been previously observed at the sites (Balland et al., 2006). The presence of

snow over vegetated targets, for example the tree that can intercept snow for longer periods, complicates the use of remote sensing and other metrics for determining spring phenology (Nelson et al., 2022). Snow cover and snow-catch efficiency do not interrupt stem-radius measurements, making them a useful and complementary tool in validation and interpretation of phenological changes approximated by other metrics.

The onset of transpiration in spring overlapped with the snowmelt in every observed year (2016–2020, five years). This shows an interesting overlap of phenological events in the boreal forest during spring, snowmelt and transpiration onset. Previous work at the studied sites (OJP and OBS) showed a strong correlation between the onset of carbon uptake and snowmelt in the spring (observations: 2011–2015) (Ahmed et al., 2021). Bowling et al. (2018) also showed that the onset of transpiration occurs during snowmelt in the Rocky Mountains. Snowmelt timing is changing (Chen et al., 2015), and snowpack is declining in northern latitudes (Mote et al., 2018; Musselman et al., 2021; Pederson et al., 2013). Thus, understanding the relationship between snowmelt and onset of transpiration in the spring is important to foresee the impact of environmental changes on vegetation phenology. Our proposed stem-temp approach provides the opportunity for a continuous and high-temporal resolution (i.e., daily) monitoring of transpiration phenology to identify phenological changes and the long-term relationship with snowmelt and climate warming impacts.

5.2. Tracking transpiration phenology: a new way forward?

We are not aware of any other technique that has evaluated the timing of phenological transition dates in tree transpiration from spring to fall. Sap flow measurements can provide an assessment of transpiration onset. Recent research has shown that one can track changes in transpiration in cold environments by developing new zero flow baselines per tree to address changes in air temperature during this period (Chan and Bowling, 2017). Sap flow sensors offer the possibility to detect transpiration but lack information on changes in storage. Thus, the detection of tree hydraulic phenology with dendrometers offers the unique opportunity to identify the timing of transpiration and storage rehydration processes in the spring. While eddy-covariance derived ET provides an indirect assessment of transpiration, ET is also influenced by understory transpiration and by snow sublimation in the spring, the latter can be a large component during the onset of the growing season (Broxton et al., 2015; Molotch et al., 2007; Sexstone et al., 2016). Thus, stem radius measurements can provide complementary information during spring onset, not observed by other methods. Future investigation should also focus on tree-to-tree variation. This could be done by monitoring stem radius and sapwood temperature simultaneously in all measured individuals. Our study was limited in this aspect as we carried the analysis based on the average species response. This information could provide transpiration phenology assessment at the individual-level.

Even though transpiration is closely linked to photosynthesis, distinct processes are captured among different measurements that can provide new perspectives on the timing of phenological changes (Pierrat et al., 2021). Thus, coupling different approaches that allow distinct assessment may improve this daunting task of defining onset and end of growing season in northern environments (Ahmed et al., 2021; Nelson et al., 2022). Additionally, phenological assessment that offers species-specific changes at daily resolution is necessary to investigate synchronicity of distinct processes and better understanding of the complex relationship with environmental drivers. This can help to detect when trees are transpiring and guide assessment of tree water use in ecosystems that goes dormant during winter (Nehemy et al., 2022) . Daily resolution assessment of transpiration phenological change is also important during shoulder seasons when there is large variability in air temperature that leads to re-freezing of stems and delays the onset of transpiration as we observed in 2017 and 2019 in this study. The observation of re-freezing of steams can be the norm rather than

exception and longer-term observations is necessary to observe this behavior. This is important with recent evidence showing that the increasing length of growing season with climate warming may lead to increased plant exposure to frost in the spring after onset of transpiration (Liu et al., 2018; Richardson et al., 2018).

6. Conclusion

We showed that the use of stem-temp approach allows a daily assessment of the timing of four transpiration phenological changes, (i) the temperature-driven cycles indicating the start of the growing season, (ii) the onset of stem rehydration, (iii) the onset of transpiration, and (iv) the end of transpiration-driven cycles indicating the end of the growing season. These phases can be both quantitatively assessed through the correlation coefficients between stem radius and stem temperature data, or stem radius and air temperature. We showed that tracking transpiration phenology using this new approach is in good agreement with canopy-level assessment of vegetation phenology through the use of Gcc. The timing of onset of transpiration observed through stem-temp assessment aligns well with observations of increase in ET, SIF, onset of net positive carbon uptake and snowmelt timing at both studied sites.

The stem-temp approach provides information about distinct processes that cannot be assessed with canopy-level phenological change measurements and is thus useful to understand species-specific phenological responses to climate warming. Phenological assessment through the use of stem radius is not affected by variable atmospheric conditions during shoulder seasons and is also not affected by canopy snow cover which limit eddy-covariance and remote sensing observations. Phenological assessment with stem radius change also offers opportunities to inform existing eddy-covariance infrastructure across North-America (e. g., FLUXNET and NEON sites) and sites with phenocams (e.g., PhenoCam Network) to improve our understanding of the links between transpiration phenology, photosynthetic phenology, and the seasonal cycles of carbon and water in northern ecosystems.

Declaration of Competing Interest

The authors declare the following financial interests/personal relationships which may be considered as potential competing interests

Data availability

I have shared the link to the data in the manuscript. We will update this links during review.

References

Ahmed, H.F., Helgason, W., Barr, A., Black, A., 2021. Characterization of spring thaw and its relationship with carbon uptake for different types of southern boreal forest. Agric. For. Meteorol. 307, 108511 https://doi.org/10.1016/j.agrformet.2021.108511.

Améglio, T., Cochard, H., Ewers, F.W., 2001. Stem diameter variations and cold hardiness in walnut trees. J. Exp. Bot. 52, 2135–2142. https://doi.org/10.1093/jexbot/52.364.2135.

Baldocchi, D.D., 2003. Assessing the eddy covariance technique for evaluating carbon dioxide exchange rates of ecosystems: past, present and future. Glob. Change Biol. 9, 479–492. https://doi.org/10.1046/j.1365-2486.2003.00629.x.

Balland, V., Bhatti, J., Errington, R., Castonguay, M., Arp, P.A., 2006. Modeling snowpack and soil temperature and moisture conditions in a jack pine, black spruce and aspen forest stand in central Saskatchewan (BOREAS SSA). Can. J. Soil Sci. 86, 203–217. https://doi.org/10.4141/S05-088.

Barichivich, J., Briffa, K.R., Myneni, R.B., Osborn, T.J., Melvin, T.M., Ciais, P., Piao, S., Tucker, C., 2013. Large-scale variations in the vegetation growing season and annual cycle of atmospheric CO2 at high northern latitudes from 1950 to 2011. Glob. Change Biol. 19, 3167–3183. https://doi.org/10.1111/gcb.12283.

Barr, A.G., Black, T.A., Hogg, E.H., Griffis, T.J., Morgenstern, K., Kljun, N., Theede, A., Nesic, Z., 2007. Climatic controls on the carbon and water balances of a boreal aspen forest, 1994–2003. Glob. Change Biol. 13, 561–576. https://doi.org/10.1111/j.1365-2486.2006.01220.x.

Barr, A.G., van der Kamp, G., Black, T.A., McCaughey, J.H., Nesic, Z., 2012. Energy balance closure at the BERMS flux towers in relation to the water balance of the White Gull Creek watershed 1999–2009. Agricultural and forest meteorology, land-atmosphere interactions: advances in measurement, analysis, and modeling – a tribute to T. Andrew Black 153, 3–13. https://doi.org/10.1016/j.agrformet.2011.05.017.

Berninger, F., 1997. Effects of drought and phenology on GPP in Pinus sylvestris: a simulation study along a geographical gradient. Funct. Ecol. 11, 33–42. https://doi.org/10.1046/j.1365-2435.1997.00051.x.

Black, T.A., Chen, W.J., Barr, A.G., Arain, M.A., Chen, Z., Nesic, Z., Hogg, E.H., Neumann, H.H., Yang, P.C., 2000. Increased carbon sequestration by a boreal deciduous forest in years with a warm spring. Geophys. Res. Lett. 27, 1271–1274. https://doi.org/10.1029/1999GL011234.

Bowling, D.R., Logan, B.A., Hufkens, K., Aubrecht, D.M., Richardson, A.D., Burns, S.P., Anderegg, W.R.L., Blanken, P.D., Eiriksson, D.P., 2018. Limitations to winter and spring photosynthesis of a Rocky Mountain subalpine forest. Agric. For. Meteorol. 252, 241–255. https://doi.org/10.1016/j.agrformet.2018.01.025.

Broxton, P.D., Harpold, A.A., Biederman, J.A., Troch, P.A., Molotch, N.P., Brooks, P.D., 2015. Quantifying the effects of vegetation structure on snow accumulation and ablation in mixed-conifer forests. Ecohydrology 8, 1073–1094. https://doi.org/10.1002/eco.1565.

Chan, A.M., Bowling, D.R., 2017. Assessing the thermal dissipation sap flux density method for monitoring cold season water transport in seasonally snow-covered forests. Tree Physiol. 37, 984–995. https://doi.org/10.1093/treephys/tpx049.

Chang, C.Y.-Y, Bräutigam, K, Hüner, N.P.A, Ensminger, I, 2021. Champions of winter survival: cold acclimation and molecular regulation of cold hardiness in evergreen conifers. New Phytol. 229, 675–691. https://doi.org/10.1111/nph.16904.

Charra-Vaskou, K., Badel, E., Charrier, G., Ponomarenko, A., Bonhomme, M., Foucat, L., Mayr, S., Améglio, T., 2016. Cavitation and water fluxes driven by ice water potential in Juglans regia during freeze–thaw cycles. J. Exp. Bot. 67, 739–750. https://doi.org/10.1093/jxb/erv486.

Charrier, G., Nolf, M., Leitinger, G., Charra-Vaskou, K., Losso, A., Tappeiner, U., Améglio, T., Mayr, S., 2017. Monitoring of freezing dynamics in trees: a simple phase shift causes complexity. Plant Physiol. 173, 2196–2207.

Chen, B., Coops, N.C., Fu, D., Margolis, H.A., Amiro, B.D., Barr, A.G., Black, T.A., Arain, M.A., Bourque, C.P.-A., Flanagan, L.B., Lafleur, P.M., McCaughey, J.H., Wofsy, S.C., 2011. Assessing eddy-covariance flux tower location bias across the Fluxnet-Canada Research Network based on remote sensing and footprint modelling. Agric. For. Meteorol. 151, 87–100. https://doi.org/10.1016/j.agrformet.2010.09.005.

Chen, B., Coops, N.C., Fu, D., Margolis, H.A., Amiro, B.D., Black, T.A., Arain, M.A., Barr, A.G., Bourque, C.P.-A., Flanagan, L.B., Lafleur, P.M., McCaughey, J.H., Wofsy, S.C., 2012. Characterizing spatial representativeness of flux tower eddy-covariance measurements across the Canadian Carbon Program Network using remote sensing and footprint analysis. Remote Sens. Environ. 124, 742–755. https://doi.org/10.1016/j.rse.2012.06.007.

Chen, X., Liang, S., Cao, Y., He, T., Wang, D., 2015. Observed contrast changes in snow cover phenology in northern middle and high latitudes from 2001 to 2014. Sci. Rep. 5, 16820. https://doi.org/10.1038/srep16820.

Chu, H., Luo, X., Ouyang, Z., Chan, W.S., Dengel, S., Biraud, S.C., Torn, M.S., Metzger, S., Kumar, J., Arain, M.A., Arkebauer, T.J., Baldocchi, D., Bernacchi, C., Billesbach, D., Black, T.A., Blanken, P.D., Bohrer, G., Bracho, R., Brown, S., Brunsell, N.A., Chen, J., Chen, X., Clark, K., Desai, A.R., Duman, T., Durden, D., Fares, S., Forbrich, I., Gamon, J.A., Gough, C.M., Griffis, T., Helbig, M., Hollinger, D., Humphreys, E., Ikawa, H., Iwata, H., Ju, Y., Knowles, J.F., Knox, S.H., Kobayashi, H., Kolb, T., Law, B., Lee, X., Litvak, M., Liu, H., Munger, J.W., Noormets, A., Novick, K., Oberbauer, S.F., Oechel, W., Oikawa, P., Papuga, S.A., Pendall, E., Prajapati, P., Prueger, J., Quinton, W.L., Richardson, A.D., Russell, E.S., Scott, R.L., Starr, G., Staebler, R., Stoy, P.C., Stuart-Haëntjens, E., Sonnentag, O., Sullivan, R.C., Suyker, A., Ueyama, M., Vargas, R., Wood, J.D., Zona, D., 2021. Representativeness of Eddy-Covariance flux footprints for areas surrounding AmeriFlux sites. Agric. For. Meteorol. 301–302, 108350 https://doi.org/10.1016/j.agrformet.2021.108350.

Commane, R., Lindaas, J., Benmergui, J., Luus, K.A., Chang, R.Y.-W., Daube, B.C., Euskirchen, E.S., Henderson, J.M., Karion, A., Miller, J.B., Miller, S.M., Parazoo, N.C., Randerson, J.T., Sweeney, C., Tans, P., Thoning, K., Veraverbeke, S., Miller, C.E., Wofsy, S.C., 2017. Carbon dioxide sources from Alaska driven by increasing early winter respiration from Arctic tundra. PNAS 114, 5361–5366. https://doi.org/10.1073/pnas.1618567114.

De Swaef, T., De Schepper, V., Vandegehuchte, M.W., Steppe, K., 2015. Stem diameter variations as a versatile research tool in ecophysiology. Tree Physiol. 35, 1047–1061. https://doi.org/10.1093/treephys/tpv080.

Drew, D.M., Downes, G.M., 2009. The use of precision dendrometers in research on daily stem size and wood property variation: a review. Dendrochronologia 27, 159–172. https://doi.org/10.1016/j.dendro.2009.06.008.

Fitzjarrald, D.R., Acevedo, O.C., Moore, K.E., 2001. Climatic consequences of leaf presence in the eastern United States. J. Clim. 14, 598–614. https://doi.org/10.1175/1520-0442(2001)014<0598:CCOLPI>2.0.CO;2.

Gamon, J.A., Huemmrich, K.F., Wong, C.Y.S., Ensminger, I., Garrity, S., Hollinger, D.Y., Noormets, A., Peñuelas, J., 2016. A remotely sensed pigment index reveals photosynthetic phenology in evergreen conifers. Proc. Natl. Acad. Sci. USA 113, 13087–13092. https://doi.org/10.1073/pnas.1606162113.

Goulden, M.L., Munger, J.W., Fan, S.-.M., Daube, B.C., Wofsy, S.C., 1996. Exchange of carbon dioxide by a deciduous forest: response to interannual climate variability. Science 271, 1576–1578.

Grossmann, K., Frankenberg, C., Magney, T.S., Hurlock, S.C., Seibt, U., Stutz, J., 2018. PhotoSpec: a new instrument to measure spatially distributed red and far-red Solar-Induced Chlorophyll Fluorescence. Remote Sens. Environ. 216, 311–327. https://doi.org/10.1016/j.rse.2018.07.002.

Guy, C.L., 1990. Cold acclimation and freezing stress tolerance: role of protein metabolism. Annu. Rev. Plant Physiol. Plant Mol. Biol. 41, 187–223. https://doi.org/10.1146/annurev.pp.41.060190.001155.

Irvine, J., Grace, J., 1997. Continuous measurements of water tensions in the xylem of trees based on the elastic properties of wood. Planta 202, 455–461. https://doi.org/10.1007/s004250050149.

Jarvis, P., Linder, S., 2000. Constraints to growth of boreal forests. Nature 405, 904–905. https://doi.org/10.1038/35016154.

Keenan, T.F., Gray, J., Friedl, M.A., Toomey, M., Bohrer, G., Hollinger, D.Y., Munger, J.W., O`Keefe, J., Schmid, H.P., Wing, I.S., Yang, B., Richardson, A.D., 2014. Net carbon uptake has increased through warming-induced changes in temperate forest phenology. Nat. Clim. Chang. 4, 598–604. https://doi.org/10.1038/nclimate2253.

King, G., Fonti, P., Nievergelt, D., Büntgen, U., Frank, D., 2013. Climatic drivers of hourly to yearly tree radius variations along a 6°C natural warming gradient. Agric. For. Meteorol. 168, 36–46. https://doi.org/10.1016/j.agrformet.2012.08.002.

Kljun, N., Black, T.A., Griffis, T.J., Barr, A.G., Gaumont-Guay, D., Morgenstern, K., McCaughey, J.H., Nesic, Z., 2006. Response of net ecosystem productivity of three boreal forest stands to drought. Ecosystems 9, 1128–1144. https://doi.org/10.1007/s10021-005-0082-x.

Kozlowski, T.T., Winget, C.H., 1964. Diurnal and seasonal variation in radii of tree stems. Ecology 45, 149–155. https://doi.org/10.2307/1937115.

Linderholm, H.W., 2006. Growing season changes in the last century. Agric. For. Meteorol. 137, 1–14. https://doi.org/10.1016/j.agrformet.2006.03.006.

Lintunen, A., Lindfors, L., Nikinmaa, E., Hölttä, T., 2017. Xylem diameter changes during osmotic stress, desiccation and freezing in Pinus sylvestris and Populus tremula. Tree Physiol. 37, 491–500. https://doi.org/10.1093/treephys/tpw114.

Liu, Q., Piao, S., Janssens, I.A., Fu, Y., Peng, S., Lian, X., Ciais, P., Myneni, R.B., Peñuelas, J., Wang, T., 2018. Extension of the growing season increases vegetation exposure to frost. Nat. Commun. 9, 426. https://doi.org/10.1038/s41467-017-02690-y.

Magney, T.S., Bowling, D.R., Logan, B.A., Grossmann, K., Stutz, J., Blanken, P.D., Burns, S.P., Cheng, R., Garcia, M.A., Köhler, P., Lopez, S., Parazoo, N.C., Raczka, B., Schimel, D., Frankenberg, C., 2019. Mechanistic evidence for tracking the seasonality of photosynthesis with solar-induced fluorescence. Proc. Natl. Acad. Sci. USA 116, 11640–11645. https://doi.org/10.1073/pnas.1900278116.

Maillet, J., Nehemy, M.F., Mood, B., Pappas, C., Bonsal, B., Laroque, C., 2022. A multi-scale dendroclimatological analysis of four common species in the southern Canadian boreal forest. Dendrochronologia 72, 125936. https://doi.org/10.1016/j.dendro.2022.125936.

Mäkinen, H., Seo, J.-.W., Nöjd, P., Schmitt, U., Jalkanen, R., 2008. Seasonal dynamics of wood formation: a comparison between pinning, microcoring and dendrometer measurements. Eur. J. For. Res. 127, 235–245. https://doi.org/10.1007/s10342-007-0199-x.

Maruta, E., Kubota, M., Ikeda, T., 2020. Effects of xylem embolism on the winter survival of Abies veitchii shoots in an upper subalpine region of central Japan. Sci. Rep. 10, 6594. https://doi.org/10.1038/s41598-020-62651-2.

Menzel, A., Fabian, P., 1999. Growing season extended in Europe. Nature 397, 659. https://doi.org/10.1038/17709, 659.

Molotch, N.P., Blanken, P.D., Williams, M.W., Turnipseed, A.A., Monson, R.K., Margulis, S.A., 2007. Estimating sublimation of intercepted and sub-canopy snow using eddy covariance systems. Hydrol. Process. 21, 1567–1575. https://doi.org/10.1002/hyp.6719.

Montgomery, R.A., Rice, K.E., Stefanski, A., Rich, R.L., Reich, P.B., 2020. Phenological responses of temperate and boreal trees to warming depend on ambient spring temperatures, leaf habit, and geographic range. Proc. Natl. Acad. Sci. 117, 10397–10405. https://doi.org/10.1073/pnas.1917508117.

Mote, P.W., Li, S., Lettenmaier, D.P., Xiao, M., Engel, R., 2018. Dramatic declines in snowpack in the western US. NPJ Clim. Atmos. Sci. 1, 1–6. https://doi.org/10.1038/s41612-018-0012-1.

Musselman, K.N., Addor, N., Vano, J.A., Molotch, N.P., 2021. Winter melt trends portend widespread declines in snow water resources. Nat. Clim. Chang. 11, 418–424. https://doi.org/10.1038/s41558-021-01014-9.

Nehemy, M.F., Maillet, J., Laroque, C., 2021. Stem radius change from Picea mariana and Larix laricina at the Old Black Spruce site, Boreal Research Ecosystem and Monitoring Sites (BERMS). Federated Research Data Repository. https://doi.org/10.20383/102.0367.

Nehemy, M.F., Maillet, J., Perron, N., Pappas, C., Sonnentag, O., Baltzer, J.L., Laroque, C. P., McDonnell, J.J., 2022. Snowmelt water use at transpiration onset: phenology, isotope tracing, and tree water transit time. Water Resour. Res. 58, e2022WR032344 https://doi.org/10.1029/2022WR032344.

Nelson, P.R., Maguire, A.J., Pierrat, Z., Orcutt, E.L., Yang, D., Serbin, S., Frost, G.V., Macander, M.J., Magney, T.S., Thompson, D.R., Wang, J.A., Oberbauer, S.F., Zesati, S.V., Davidson, S.J., Epstein, H.E., Unger, S., Campbell, P.K.E., Carmon, N., Velez-Reyes, M., Huemmrich, K.F., 2022. Remote sensing of tundra ecosystems using high spectral resolution reflectance: opportunities and challenges. J. Geophys. Res.: Biogeosci. 127, e2021JG006697 https://doi.org/10.1029/2021JG006697.

Pappas, C., Maillet, J., Rakowski, S., Baltzer, J.L., Barr, A.G., Black, T.A., Fatichi, S., Laroque, C.P., Matheny, A.M., Roy, A., Sonnentag, O., Zha, T., 2020. Aboveground tree growth is a minor and decoupled fraction of boreal forest carbon input. Agric. For. Meteorol. 290, 108030 https://doi.org/10.1016/j.agrformet.2020.108030.

Parazoo, N.C., Arneth, A., Pugh, T.A.M., Smith, B., Steiner, N., Luus, K., Commane, R., Benmergui, J., Stofferahn, E., Liu, J., Rödenbeck, C., Kawa, R., Euskirchen, E., Zona, D., Arndt, K., Oechel, W., Miller, C., 2018. Spring photosynthetic onset and net CO_2 uptake in Alaska triggered by landscape thawing. Glob. Chang. Biol. 24, 3416–3435. https://doi.org/10.1111/gcb.14283.

Parazoo, N.C., Magney, T., Norton, A., Raczka, B., Bacour, C., Maignan, F., Baker, I., Zhang, Y., Qiu, B., Shi, M., MacBean, N., Bowling, D.R., Burns, S.P., Blanken, P.D., Stutz, J., Grossmann, K., Frankenberg, C., 2020. Wide discrepancies in the magnitude and direction of modeled solar-induced chlorophyll fluorescence in response to light conditions. Biogeosciences 17, 3733–3755. https://doi.org/10.5194/bg-17-3733-2020.

Pederson, G.T., Betancourt, J.L., McCabe, G.J., 2013. Regional patterns and proximal causes of the recent snowpack decline in the Rocky Mountains, U.S. Geophys. Res. Lett. 40, 1811–1816. https://doi.org/10.1029/2022WR032344.

Peng, S., Ciais, P., Chevallier, F., Peylin, P., Cadule, P., Sitch, S., Piao, S., Ahlström, A., Huntingford, C., Levy, P., Li, X., Liu, Y., Lomas, M., Poulter, B., Viovy, N., Wang, T., Wang, X., Zaehle, S., Zeng, N., Zhao, F., Zhao, H., 2015. Benchmarking the seasonal cycle of CO2 fluxes simulated by terrestrial ecosystem models. Glob. Biogeochem. Cycles 29, 46–64. https://doi.org/10.1002/2014GB004931.

Perämäki, M., Nikinmaa, E., Sevanto, S., Ilvesniemi, H., Siivola, E., Hari, P., Vesala, T., 2001. Tree stem diameter variations and transpiration in Scots pine: an analysis using a dynamic sap flow model. Tree Physiol. 21, 889–897. https://doi.org/10.1093/treephys/21.12-13.889.

Pierrat, Z., Magney, T., Parazoo, N.C., Grossmann, K., Bowling, D.R., Seibt, U., Johnson, B., Helgason, W., Barr, A., Bortnik, J., Norton, A., Maguire, A., Frankenberg, C., Stutz, J., 2022. Diurnal and seasonal dynamics of solar-induced chlorophyll fluorescence, vegetation indices, and gross primary productivity in the boreal forest. J. Geophys. Res.: Biogeosci. 127, e2021JG006588 https://doi.org/10.1029/2021JG006588.

Pierrat, Z., Nehemy, M.F., Roy, A., Magney, T., Parazoo, N.C., Laroque, C., Pappas, C., Sonnentag, O., Grossmann, K., Bowling, D.R., Seibt, U., Ramirez, A., Johnson, B., Helgason, W., Barr, A., Stutz, J., 2021. Tower-based remote sensing reveals mechanisms behind a two-phased spring transition in a mixed-species boreal forest. J. Geophys. Res.: Biogeosci. 126, e2020JG006191 https://doi.org/10.1029/2020JG006191.

Pierrat, Z., Stutz, J. Tower-based solar-induced fluorescence and vegetation index data for Southern Old Black Spruce forest [Data set]. Zenodo. https://doi.org/10.5281/zenodo.5884643.

Rajashekar, C., Burke, M.J., 1982. Liquid water during slow freezing based on cell water relations and limited experimental testing. Eds.. In: Li, P.H., Sakai, A. (Eds.), Plant

Cold Hardiness and Freezing Stress. Academic Press, pp. 211–220. https://doi.org/10.1016/B978-0-12-447602-8.50021-0.

Richardson, A.D., Anderson, R.S., Arain, M.A., Barr, A.G., Bohrer, G., Chen, G., Chen, J. M., Ciais, P., Davis, K.J., Desai, A.R., Dietze, M.C., Dragoni, D., Garrity, S.R., Gough, C.M., Grant, R., Hollinger, D.Y., Margolis, H.A., McCaughey, H., Migliavacca, M., Monson, R.K., Munger, J.W., Poulter, B., Raczka, B.M., Ricciuto, D. M., Sahoo, A.K., Schaefer, K., Tian, H., Vargas, R., Verbeeck, H., Xiao, J., Xue, Y., 2012. Terrestrial biosphere models need better representation of vegetation phenology: results from the North American carbon program site synthesis. Glob. Chang. Biol. 18, 566–584. https://doi.org/10.1111/j.1365-2486.2011.02562.x.

Richardson, A.D., Andy Black, T., Ciais, P., Delbart, N., Friedl, M.A., Gobron, N., Hollinger, D.Y., Kutsch, W.L., Longdoz, B., Luyssaert, S., Migliavacca, M., Montagnani, L., William Munger, J., Moors, E., Piao, S., Rebmann, C., Reichstein, M., Saigusa, N., Tomelleri, E., Vargas, R., Varlagin, A., 2010. Influence of spring and autumn phenological transitions on forest ecosystem productivity. Philos. Trans. R. Soc. B: Biol. Sci. 365, 3227–3246. https://doi.org/10.1098/rstb.2010.0102.

Richardson, A.D., Hufkens, K., Milliman, T., Aubrecht, D.M., Chen, M., Gray, J.M., Johnston, M.R., Keenan, T.F., Klosterman, S.T., Kosmala, M., Melaas, E.K., Friedl, M. A., Frolking, S., 2018. Tracking vegetation phenology across diverse North American biomes using PhenoCam imagery. Sci. Data 5, 180028. https://doi.org/10.1038/sdata.2018.28.

Richardson, A.D., Keenan, T.F., Migliavacca, M., Ryu, Y., Sonnentag, O., Toomey, M., 2013. Climate change, phenology, and phenological control of vegetation feedbacks to the climate system. Agric. For. Meteorol. 169, 156–173. https://doi.org/10.1016/j.agrformet.2012.09.012.

Schwartz, M.D., Crawford, T.M., 2001. Detecting energy-balance modifications at the onset of spring. Phys. Geogr. 22, 394–409. https://doi.org/10.1080/02723646.2001.10642751.

Sevanto, S., Suni, T., Pumpanen, J., Grönholm, T., Kolari, P., Nikinmaa, E., Hari, P., Vesala, T., 2006. Wintertime photosynthesis and water uptake in a boreal forest. Tree Physiol. 26, 749–757. https://doi.org/10.1093/treephys/26.6.749.

Sexstone, G.A., Clow, D.W., Stannard, D.I., Fassnacht, S.R., 2016. Comparison of methods for quantifying surface sublimation over seasonally snow-covered terrain. Hydrol. Process. 30, 3373–3389. https://doi.org/10.1002/hyp.10864.

Seyednasrollah, B., Bowling, D.R., Cheng, R., Logan, B.A., Magney, T.S., Frankenberg, C., Yang, J.C., Young, A.M., Hufkens, K., Arain, M.A., Black, T.A., Blanken, P.D., Bracho, R., Jassal, R., Hollinger, D.Y., Law, B.E., Nesic, Z., Richardson, A.D., 2021. Seasonal variation in the canopy color of temperate evergreen conifer forests. New Phytol. 229, 2586–2600. https://doi.org/10.1111/nph.17046.

Seyednasrollah, B., Young, A.M., Hufkens, K., Milliman, T., Friedl, M.A., Frolking, S., Richardson, A.D., 2019. Tracking vegetation phenology across diverse biomes using Version 2.0 of the PhenoCam Dataset. Sci. Data 6, 222. https://doi.org/10.1038/s41597-019-0229-9.

Sonnentag, O., Hufkens, K., Teshera-Sterne, C., Young, A.M., Friedl, M., Braswell, B.H., Milliman, T., O'Keefe, J., Richardson, A.D., 2012. Digital repeat photography for phenological research in forest ecosystems. Agric. For. Meteorol. 152, 159–177. https://doi.org/10.1016/j.agrformet.2011.09.009.

Steppe, K., De Pauw, D.J.W., Lemeur, R., Vanrolleghem, P.A., 2006. A mathematical model linking tree sap flow dynamics to daily stem diameter fluctuations and radial stem growth. Tree Physiol. 26, 257–273. https://doi.org/10.1093/treephys/26.3.257.

Tardif, J., Flannigan, M., Bergeron, Y., 2001. An analysis of the daily radial activity of 7 boreal tree species, northwestern Quebec. Environ. Monit. Assess. 67, 141–160. https://doi.org/10.1023/A:1006430422061.

Turcotte, A., Morin, H., Krause, C., Deslauriers, A., Thibeault-Martel, M., 2009. The timing of spring rehydration and its relation with the onset of wood formation in black spruce. Agric. For. Meteorol. 149, 1403–1409. https://doi.org/10.1016/j.agrformet.2009.03.010.

Vitasse, Y., Signarbieux, C., Fu, Y.H., 2018. Global warming leads to more uniform spring phenology across elevations. PNAS 115, 1004–1008. https://doi.org/10.1073/pnas.1717342115.

Walther, S., Guanter, L., Heim, B., Jung, M., Duveiller, G., Wolanin, A., Sachs, T., 2018. Assessing the dynamics of vegetation productivity in circumpolar regions with different satellite indicators of greenness and photosynthesis. Biogeosciences 15, 6221–6256. https://doi.org/10.5194/bg-15-6221-2018.

Wolf, S., Keenan, T.F., Fisher, J.B., Baldocchi, D.D., Desai, A.R., Richardson, A.D., Scott, R.L., Law, B.E., Litvak, M.E., Brunsell, N.A., Peters, W., van der Laan-Luijkx, I. T., 2016. Warm spring reduced carbon cycle impact of the 2012 US summer drought. Proc. Natl. Acad. Sci. USA 113, 5880–5885. https://doi.org/10.1073/pnas.1519620113.

Wu, C., Chen, J.M., Black, T.A., Price, D.T., Kurz, W.A., Desai, A.R., Gonsamo, A., Jassal, R.S., Gough, C.M., Bohrer, G., Dragoni, D., Herbst, M., Gielen, B., Berninger, F., Vesala, T., Mammarella, I., Pilegaard, K., Blanken, P.D., 2013. Interannual variability of net ecosystem productivity in forests is explained by carbon flux phenology in autumn. Glob. Ecol. Biogeogr. 22, 994–1006. https://doi.org/10.1111/geb.12044.

Wutzler, T., Lucas-Moffat, A., Migliavacca, M., Knauer, J., Sickel, K., Šigut, L., Menzer, O., Reichstein, M., 2018. Basic and extensible post-processing of eddy covariance flux data with REddyProc. Biogeosciences 15, 5015–5030. https://doi.org/10.5194/bg-15-5015-2018.

Young-Robertson, J.M., Bolton, W.R., Bhatt, U.S., Cristóbal, J., Thoman, R., 2016. Deciduous trees are a large and overlooked sink for snowmelt water in the boreal forest. Sci. Rep. 6, 29504. https://doi.org/10.1038/srep29504.

Zhang, T., 2005. Influence of the seasonal snow cover on the ground thermal regime: an overview. Rev. Geophys. 43 https://doi.org/10.1029/2004RG000157.

Zweifel, Haeni, M., Buchmann, N., Eugster, W., 2016. Are trees able to grow in periods of stem shrinkage? New Phytol. 211, 839–849. https://doi.org/10.1111/nph.13995.

Zweifel, R., Eugster, W., Etzold, S., Dobbertin, M., Buchmann, N., Häsler, R., 2010. Link between continuous stem radius changes and net ecosystem productivity of a subalpine Norway spruce forest in the Swiss Alps. New Phytol. 187, 819–830.

Zweifel, R., Hasler, R., 2001. Dynamics of water storage in mature subalpine Picea abies: temporal and spatial patterns of change in stem radius. Tree Physiol. 21, 561–569. https://doi.org/10.1093/treephys/21.9.561.

Zweifel, R., Häsler, R., 2000. Frost-induced reversible shrinkage of bark of mature subalpine conifers. Agric. For. Meteorol. 102, 213–222. https://doi.org/10.1016/S0168-1923(00)00135-0.